A STATISTICAL METHOD OF FOG FORECASTING IN NORTH CAROLINA

by

Warren Eugene Pettee

A thesis submitted to the faculty of
The University of North Carolina at Charlotte
in partial fulfillment of the requirements
for the degree of Master of Science in
Earth Science

Charlotte

2018

Approved by:

_____
Dr. Matthew Eastin

_____
Dr. Brian Magi

_____
Terry Shirley

ABSTRACT

WARREN EUGENE PETTEE. A Statistical Method of Fog Forecasting in North Carolina. (Under the direction of DR. MATTHEW D. EASTIN)

The frequency and intensity at which fog occurs impacts the entire transportation infrastructure of the United States: Maritime shipping, aviation, railroads, and highways. The phenomenon is difficult to accurately capture in current numerical simulation forecasts, which places the burden of fog detection on observation-based statistical methods. This project explores a method of forecasting fog using combined probabilities generated from 40-yr event based climatologies of several variables. The final probabilities are too small to serve as a standalone tool but do show promise in serving as a foundation for further development as a forecaster.

TABLE OF CONTENTS

LIST OF FIGURES

LIST OF ABBREVIATIONS

AMS   American Meteorological Society

ASOS   Automated Surface Observing System

CSV   Comma-Separated Values

EST   Eastern Standard Time

GOES   Geostationary Operational Environmental Satellite

NC   North Carolina

NOAA   National Oceanic and Atmospheric Administration

WRF   Weather Research and Forecasting model

Chapter 1: Introduction

The frequency and intensity at which fog occurs impacts the entire transportation infrastructure of the United States: Maritime shipping, aviation, railroads, and highways. The Federal Highway Administration estimates that there are over 5.5 million vehicle crashes every year, about 20 percent of these crashes are related to adverse weather conditions (2002-2012). North Carolina is especially prone; the state spans from a flat coastal plain, subject to many maritime fog effects, to the Appalachian Mountains, a range well known for producing deadly mountain-valley fog. Between 2002 and 2012, 19,188 vehicle crashes were related to fog in North Carolina (Oliver 2013). The phenomenon is difficult to capture in current computer forecasting techniques, which places the burden of fog detection on observation-based statistical methods.

Fog forecasting presents a major challenge for meteorologists, this project seeks to explore a combined probability method where fog-conducive variables are extracted from climatology data and used in an event-based climatology for building single variable probabilities. The primary goal is to offer a method that is lower in cost compared to numerical modeling and with a smaller infrastructure footprint than other methods.

1.1: Defining Fog

The American Meteorological Society (AMS) Glossary defines fog as "water droplets suspended in the atmosphere in the vicinity of the earth's surface that affect visibility". Fog is attributed when horizontal visibility is reduced to below 1 km, and generally forms when the temperature and dewpoint are equal in value (i.e., saturation, AMS 2015). Fog may form when the temperature is cooled to saturation or when a moisture source increases the dewpoint to saturation. The AMS Glossary further states that fog

rarely forms when the difference between the temperature and dewpoint are greater than 4°F. Additional subcategories of fog are also defined to address the vertical component of fog: Fog that allows vision 6 ft above the surface is defined as shallow fog, and if the sky is not concealed more than 60% (0.6) then this is defined as ground fog. A special case is when fog consists primarily of ice crystals instead of water droplets, in this case it is termed ice fog. Fog occurs in the lowest portions of the atmosphere, within the planetary boundary layer. There are several varieties of fog, each with their own unique methods of formation.

Radiation fog makes up the vast majority of fog cases. It forms during the rapid cooling of the surface after sunset, or during maximum radiational cooling. Favorable conditions are 1) a shallow surface layer of relatively moist air beneath a dry layer and clear skies, and 2) light surface winds (AMS 2015). Additionally, fog may form when moist air passes over a cooler surface, termed advection fog. This commonly occurs over cooler bodies of water where it may be termed sea fog. Steam fog is a variety that appears when cooler air passes over warmer waters. More generally, it forms when "water vapor is added to air that is much colder than the vapor's source" (AMS 2015). This variety is unique in that it is a convective phenomenon, often creating lower visibility situations than the aforementioned varieties.

All types of fog may also become forms of ice fog or freezing fog if conditions are correct. Ice fog types consist of ice crystals instead of water droplets (AMS 2015). Freezing fog, another variety, consists of supercooled water droplets that often freeze to surfaces on contact, creating a dangerous situation for transportation infrastructure. Supercooled water droplets, in the context of freezing fog, are a threat when temperatures are below freezing but above the ice crystal growth region.

1.2: Fog Formation

The common ground for all types of fog is in how it forms, fog tends to form in light winds, when the temperature decreases to saturation or when the dewpoint increases to saturation, and there is an adequate moisture source (AMS 2015). Previous synoptic climatologies of fog for a region (e.g., Meyer and Lala 1990), found that most radiation fog forms when $\frac{\partial T}{\partial t} < 0.25 \ \frac{°C}{hr}$, $-7.6°C < T < 17.5°C$, and wind speed is $< 3.1 \ m \ s^{-1}$. The sun also serves to both enhance and dissipate the fog. It was found that fog is commonly observed in the hour before and after sunrise until the solar heating induces sufficient mixing to cause dissipation.

Topography must also be considered for a project in North Carolina, as the western portion is dominated by the Appalachian range. Flow in the direction of topography will create an area of stagnation near the base (Golding, 1993). A drainage flow may form down the slope that creates an area of convergence at the surface near the stagnation. These motions seem to play a role in the formation of Appalachian fog, and at a smaller scale in the low valleys of western North Carolina.

A recent study demonstrated the use of an event-based climatology of fog to present the frequency of fog occurrence (Tardif and Rasmussen, 2007). Fog cases were categorized by type and time of occurrence before the types were compared to the total fog occurrences. This event-based frequency method demonstrated the prevalence of fog types around the New York City area.

1.3: Observation of Fog

The observation of fog is straightforward. Based on the AMS definition, any visibility less than 1 km is termed fog. The Automated Surface Observing System (ASOS) instrument used to measure fog is a forward scatter meter (ASOS, 1998). Visibility is a subjective observation; however, the National Weather Service has attempted to find objective ways to measure it. The concept of Sensor Equivalent Visibility was derived to fill this gap by measuring the forward scattering in a 0.75 cu ft sample of air. The algorithm used at ASOS stations first collects a 1-minute average extinction coefficient every minute for 10 minutes, and then calculates a 10-minute harmonic mean every minute. The harmonic mean is responsive to deteriorating visibility and under-estimates the visibility but is slower in reporting improving visibility. These methods are used in the interest of aviation safety, as the output from these stations are most immediately used for aircraft.

ASOS stations are located inconsistently across North Carolina, and rarely in fog prone regions since they represent areas not conducive to airport operations. Not all weather stations use instruments that can measure the horizontal visibility, both due to physical and financial constraints. Thus, there is merit in the early detection of fog with more rudimentary instrumentation. Fog is largely dependent on the saturation of air; however, most consumer-level sensors are not capable of fully measuring saturation or supersaturation but can read a maximum of 99% humidity (Gerber 1981). There is evidence that air can achieve supersaturation during a fog event, however by definition this cannot occur before the fog occurs. Thus, the burden for detecting fog at or before the onset of an event falls on other variables available from most weather stations (i.e. temperature, dewpoint, wind speed, wind direction).

1.4: Satellite Technologies

Satellites offer a unique point of view for near real time fog detection, but some challenges prevent its use in forecasting. Satellites lack an ability to distinguish fog from low-altitude stratus (Westcott 2007). The difference is important since one (fog) reduces ground visibility to dangerous levels and the other (low-altitude stratus) does not. Additionally, the infrared bands from the Geostationary Operational Environmental Satellites (GOES) are unable to distinguish shallow fog from clear air at night when the temperature difference between the two is small (Ellrod 1995). Night observations tend to be impaired by inversions above the fog layer and clouds above the fog layer (Ellrod, 2002). Modern detection algorithms have improved, but one such algorithm only has increased effectiveness when high and mid-level cloud cases are removed (Gultepe, 2007). The temperature difference between the satellite-estimated surface temperature and surface observations can be as large as 2°C, which severely limits satellite-based efforts with the early detection of fog. As of late 2017, the GOES-16 satellite began providing views of the western hemisphere at unprecedented spatial resolutions, but any benefit to fog detection has yet to be realized. It is also important to note that while satellites might be able to detect fog after it forms, it is unlikely they will serve as a prognostic tool for fog detection. These inadequacies place most of the burden of early fog detection on existing surface observing stations and any strategic expansion of such networks into fog-prone regions.

1.5: Modeling Fog

Accurately simulating fog within numerical models is often reserved for research studies. There is at least one case where operational numerical model output has been evaluated as an effective predictor of fog in the Yellow Sea region of China (Zhou and Du,

2010). The study used a multi-variable diagnostic fog detection technique developed at the National Center for Atmospheric Research applied to a multi-member ensemble of Weather Research and Forecasting (WRF) simulations at 15-km grid spacing. The study found that the multi-variable approach to diagnosing fog far outperforms the traditional "liquid water content (LWC) only" approach, and that the effectiveness is further improved by introducing the technique into an ensemble environment. The equitable threat score (ETS) of the LWC-only approach was only 0.063 when compared to the multi-variable approach where the ETS was 0.225. In the ensemble environment, the study calculated an ETS of 0.334. While promising, the multi-variable technique introduced in the study simply identifies the presence of fog and not the intensity.

Another study used the WRF model under several variations of microphysics and boundary layer schemes and compared it to the High-Resolution Limited-Area Model (HIRLAM) to forecast radiation fog induced by frost (van der Velde et al. 2010). The study concluded by offering that although the WRF could not capture dissipation and onset very well, it did capture the mean variables (van der Velde et al. 2010).

Despite improvements in modeling techniques, very small resolutions are often required to adequately detect fog-pone regions, which requires extensive dedicated computing resources. For remote regions and institutions unable to justify allocating the required resources, modeling does not appear to be a viable solution. This, again, brings the focus back to observation-based methods.

1.6: Building a Technique for Single Sites

Prior research largely addresses climatologies and modeling cases. In this project, we have built on the results of these climatologies and introduced them to the sites of interest. After acquiring site data, multiple variables related to fog onset, longevity, intensity, and dissipation were verified in exhibiting similar behavior as identified by prior research. All variables at each site were then summarized in terms of fog prevalence to help establish an event-based climatology following the methods outlined in Tardif and Rasmussen (2007). However, this project simplifies the climatology by focusing only on whether fog occurs (or not) during a given month and time of day (i.e., not by classifying the fog type). Unlike previous research, the resulting frequencies of each forecast variable in the event climatology were combined and evaluated as a prognostic tool.

Chapter 2: Data and Methodology

To satisfy the requirement for a simple and cost-effective solution, long-term datasets from select ASOS sites were used to build a climatology of fog in North Carolina. From the datasets, the variables were extracted and used to construct probability tables to aid in the diagnosis of fog formation.

Three stations in North Carolina have been selected for study: New Bern, NC (Coastal), Greensboro, NC (Piedmont), and Asheville, NC (Mountains). The sites were selected based on the longevity of their observations, integrity of the maintaining authority, and their representativeness of the three major terrain types across North Carolina (coastal, piedmont, and mountains). The eastern coastal region is composed of low-lying, generally-flat terrain often influenced by diurnal coastal circulations (i.e., sea breezes and advection fog) , while the central piedmont region is composed of gentle rolling hills and wide valleys with no dominant local circulations, and the western mountain region is defined by mountains and deep valleys where local weather is often influenced by diurnal mountain-valley circulations – all three regions are influenced by transient synoptic-scale weather systems. The final results assess the ability for a statistical method to detect fog across the entire state of North Carolina, thus the need to assess the three distinct regions. The diverse environments build integrity into the results, but also present challenges in building a dataset capable of detecting fog with perfect accuracy. Figure 1 provides a geographic overview of the three sites of interest.

To provide long-term statistics, ASOS data from the Iowa Environmental Mesonet ASOS archive was downloaded. The data was used to build 40-yr monthly and diurnal fog event databases with statistics generated from 1974 to 2014.

The Iowa Environmental Mesonet ASOS archive represents raw observations that have been minimally quality controlled outside of their controlling agency. Much of the concerns of observation integrity have been mitigated by only using the ASOS network, which is quality controlled by NOAA. Data was obtained in CSV format from 1 January 1974 to 31 December 2014 to ensure that all observations were NOAA quality controlled..

A "fog event" was defined as any sequential series of hourly observations with visibility less than 0.62 miles and fog reported as the observed weather. Only fog was accepted as a present weather code as opposed to rain-fog or snow-fog. This likely biased the final results towards fog cases not occurring in the presence of precipitation. Snow cover was also not incorporated in the analysis, which omits advective events induced by the snow cover.

Each fog case was identified by a beginning, peak, and end, where the peak was defined as the time with the lowest visibility between the start and end. The start of a new fog event was required to have at least 6 hours of fog-free conditions after the end of the previous fog event. This latter criterion prevents the over-detection of events that subside and reappear several times throughout the day.

One difficulty in classifying events for this project was that there are no formally defined time spans for day, evening, night, or morning. Official times such as sunrise or civil twilight are poor boundaries for considering the occurrence of fog since an event can start before sunrise and persist into the mid-morning. Thus, four broad time intervals were defined based on the average time of sunrise, sunset, and solar noon. In the region of interest (North Carolina) these times vary by approximately 3 hours annually. The time spans were determined using the equinox sunset/sunrise hour of 7 AM and 7 PM as an

approximate median for 6-h intervals of morning and evening respectively, resulting in the following time intervals for morning (5 AM – 10 AM), day (11AM – 4 PM), evening (5 PM – 10 PM) and night (11 PM – 4 AM).

After the data was acquired, it was parsed for each site to build a detailed climatology of fog. Asheville, Greensboro, and New Bern have 2696, 1117, and 1572 fog events, respectively, in their climatologies. For each fog occurrence, the following variables were tabulated: previous 6-h, 12-h, and 24-h precipitation totals, 6-h change in temperature, 6-h change in dewpoint depression, wind speed, and wind direction. Then, monthly histograms were constructed for each variable during each fog event and summarized using box-whisker plots (whereby the boxes that represent the interquartile range, the centerline denotes the median, the whiskers represent the 10th and 90th percentiles, and dots represent outliers). Anomalies with respect to a mean diurnal cycle for each variable were initially investigated but subsequently omitted because the changes in anomalies were similar to the observed changes (i.e., normalizing by the mean diurnal cycle did not provide additional clarity).

After the preliminary information was gathered, bin ranges and intervals were defined for each variable. For example, the 6-h temperature change bins started at -2.0ºF and continued every 0.25ºF degrees to +2.0ºF, which included the -0.25ºC (-0.9°F) rate threshold identified by Meyer and Lala (1990) while also allowing for outliers to be introduced. The 6hr change in dewpoint depression used the same bins as the temperature, since the bins were evenly spaced and recognizing that environments will be near saturation for fog to occur. Wind speed was binned from 0 to 10mph every 2mph. Wind direction was divided into equal-interval 45º bins (with 0 serving as its own bin for calm conditions),

while precipitation was divided into non-equal-interval bins to better capture its logarithmic distribution (bin boundaries were defined by 0.00, 0.01, 0.05, 0.1, 0.2, 0.3, 0.4, 0.5, 0.75, 1.0, 1.25, 1.5, 1.75, and 2.00 inches, respectively, with all amounts greater than 2.00 inches included in the last bin).

Based on the bins defined above, all variables during fog events were tabulated for morning, day, evening, night, and into a "all day" monthly category (i.e., regardless of the time of day). The process was repeated a second time using all hours of every day (regardless of fog formation) for each site to create a 40-yr climatology for each site. These two histogram sets (displayed as histograms), along with the preliminary precipitation analysis (displayed as box-whisker graphs), are shown in Figures 2 - 20 for each site.

Following methods outlined in Tardif and Rasmussen (2007), the climatology bins were used to create frequencies. Because this project's conclusion will test these frequencies as predictors, the frequencies will be referred to as probabilities from here forward.

The number of fog cases per bin were divided by the total dates contributing to the bin to create a 40-yr probability of fog formation. The bins and the probabilities were then combined into data tables in the CSV format. Probability tables were selected to be the final product for detecting fog due to their ease of interpretation by end users. Next, the generated probabilities were assessed by cycling back through the dataset and identifying fog observations based on the same fog event criteria above. More precise quality control was used in this test: all variables used in the probability table were required to have no missing observations. This reduced the sample size from 2696 to 927 in Asheville, from 1117 to 821 in New Bern, and from 1572 to 323 in Greensboro.

The observed variables were identified by bin and the matching probability for the observation was found from the table. The values were then multiplied together to create a combined climatology probability. These probabilities were saved as a function of month, time of day, and whether (or not) fog occurred.

To help assess the utility of these combined climatology probabilities, the 75th percentile of probabilities in cases where fog did not occur (referred to as false alarms) was found. This was used to find the percent of the total true fog forecasts that exceeded the false alarm 75th percentile threshold probability. This was repeated for each month and time of day at each site.

Chapter 3: Results

The initial climatology results are depicted by site in Figures 2 through 17, along with an accompanying map of the sites and geography in Figure 1. Figures 3, 4, and 5 depict annual wind roses for all observations (These images are courtesy of the Iowa Environmental Mesonet). Asheville, Greensboro, and New Bern have a fog case sample sizes of 2696, 1117, and 1572, respectively, in these preliminary plots.

The wind roses at all sites (see Figure 2) presented evidence of a directional component more favorable to fog formation. For example, during November through February in Greensboro fog formation was more prevalent during periods with southeasterly winds. The mean wind directions in those months range from southerly to northwesterly (Figure 3), which is consistent with the mean flow for the region. The southeasterly component is not surprising given the need for moisture and/or warmer air for fog to form. The southeasterly prevalence subsides from spring through fall, giving way for another favorable fog-supporting pattern with prevailing winds from the north and northeast. For example, in May, the mean wind is southeasterly, but the strongest signal for fog is out of the northeast. This could indicate cool, moist winds out of the northeast, but summer months are difficult to quantify because of the lower sample size.

New Bern exhibited a wintertime northerly wind component for fog formation. On average, wind in New Bern is out of the north or west (Figure 4). Wind speeds were at 2-5 mph, which contrasts with Greensboro's largely calm winds. This could be indicative of an advective component to fog formation in New Bern, since moisture may already be in place in this maritime environment.

Asheville shows a strong north or south wind component year-round, which is also present in the mean wind (Figure 5). This could demonstrate an orographic contribution to fog formation in Asheville due to the north-south orientation of the valley. This is only discernable in some winter months where there is a strong southerly signal, which contrasts with the primarily northerly direction of the mean wind. The northerly component could point to orographic influences, like those mentioned in Golding (1993), where a drainage flow forms down a slope and creates an area of convergence at the surface. Further research would be required to determine if there is a significant orographic effect in Asheville due to the mean wind also having strong north-south wind components.

Meyer and Lala (1990) found that fog generally forms when the rate of temperature change is less than 0.9°F/hr. In looking at the 6-hr temperature change histograms (Figures 6-9), it is clear that the previous study can be extended to other fog types and regions. In Greensboro, all fog scenarios except one had the highest final probabilities within the criteria from the previous study. The outlier in Greensboro was in the daytime January category with a high probability (7.69%) derived from 1 fog case and 13 non-fog cases. The second highest probability in that category was within the Meyer and Lala criteria with a probability of 1.37% derived from 2 fog cases and 146 observations. Asheville has a similar pattern, with all categories but five falling in-line with the criteria. In Asheville, the outlier was September nights with temperature changes from -1.25 to -1.00 F/hr with a probability of 9.26% (derived from 66 fog cases and 712 observations). New Bern was similarly within the criteria for 48 of the 60 temporal categories. Most of the outliers were due to low case numbers, however three were in the night -1.25 to -1.00 F/hr bin category with event totals greater than 10; April (2.4%), October (6.4%), and November (5.1%).

The 6-hour rate of change of dewpoint depression had its highest probabilities between the ranges of 0.00 to -0.75 °F/hr prior to fog onset. In Asheville fog probabilities were within this range for 52 of 60 categories, with 6 of the 8 outliers taking place in the evening between May and November when there are very few total fog cases. In Greensboro, 55 of 60 categories were between 0.00 to -0.75 °F/hr prior to fog onset. Four of the five outliers had probabilities of zero, and one of the five outliers was for daytime November fog (with a probability of 4.54% derived from 1 fog case and 22 observations). New Bern had 48 of 60 categories with the highest probabilities in the range of 0.00 to - 0.75 °F/hr. Seven of the 12 outliers had probabilities of zero. The overall range would indicate that cooling to dewpoint occurs in most fog cases at these sites. Most sites do have a small number of observed cases indicating a positive dewpoint depression. This could be a false signal from events that started and ended within the same hour. Fog case histograms are depicted in figures 9 through 10.

In Asheville and Greensboro, the precipitation preceding fog onset generally shows less precipitation in the 6 hours prior to a fog event than in the 12 and 24 hours preceding. In Asheville, 6-hour totals (Figure 12) are less than 0.5 inches with outliers in the evening and night of January, April, and October. The 12-hour precipitation (Figure 13) is more varied, but with totals generally less than one inch. The 24-hour precipitation (Figure 14) is less confined with several cases throughout the year with totals over one inch. The 6-hour precipitation totals in Greensboro (Figure 15) are similar to those in Asheville, with most hours throughout the year having less than 0.5 inches. However, in Greensboro there are 7 hours throughout the year in excess of 0.5 inches and 3 hours with totals in excess of 1 inch. The 12-hour precipitation totals (Figure 16) are mostly under one inch, like in

Asheville, while the 24-hour precipitation (Figure 17) shows many cases with precipitation over 1 inch. New Bern shows a much different 6-hour precipitation trend (Figure 18), with most hours having zero precipitation. However, outlier hours were mostly less than 0.5 inches, like at the other sites, with only one outlier near 0.75 inches. The 12-hour precipitation (Figure 19) is similarly sparse when compared to the other sites, with few cases showing precipitation in excess of 1 inch. The 24-hour precipitation totals (Figure 20) are similar to the 12 hour, with totals rarely exceeding 1 inch. In both the 12- and 24-hour precipitation figures, measurable precipitation occurred from 8PM to 5AM EST. Fog events at all locations can occur after precipitation events, since the events themselves bring a low-level moisture source for fog. Because of the strong cooling signals shown in the temperature change histograms, this could also indicate a tendency for strong radiative cooling behind precipitation events that induce fog. New Bern was the outlier site, showing a preference for precipitation to precede fog in the evening and early morning hours.

The combined event-based climatology probabilities are depicted in Figures 18 through 20. These box plots show the distribution of monthly forecast probabilities for fog cases and false alarms for morning, day, evening, and night. A value is shown as a false alarm when there was a probability greater than zero but no fog. In the figures, the values are scaled as "nano-percents" (10^{-9}) because the probabilities are much less than one. The choice to scale the results was to improve plotting readability when a 12-month plot is shown, like in other figures. Because the observation requirements were more stringent, the sample sizes were drastically reduced for the three sites: 927 for Asheville, 323 for Greensboro, and 821 for New Bern. The 75th percentile of false alarm probabilities was less than the median of observed fog probabilities at all sites for most months. Greensboro

(Figure 21) has a few exceptions: September and May mornings had higher false alarm probabilities than observed fog. Asheville (Figure 22) also had exceptions in September, June, August, and September mornings when the 75th percentile of false alarm probabilities were higher than the median of observed fog probabilities.

The percent of observed fog cases detected, if 75th percentile probability value from the false alarms is used as a minimum valid probability threshold, is shown in figures 24, 26, and 28. Companion figures 25, 27, and 29 show the corresponding sample sizes. In Asheville (Figure 24) only 3 months of the year would identify more than 50 percent of actual morning fog observations;100% of day cases are identified in December, but the day case sample size (Figure 25) for December is less than 10. Night cases identify over 50% of actual fog observations in April and December. Greensboro (Figure 26) has more scenarios where more than 50% of fog cases are accurately identified. January evenings and nights, February mornings and evenings, and March mornings and evenings identify more than 50% of fog cases. April through June have sample sizes (Figure 27) less than 5 but high identification rates. July through December offer identification rates greater than 35% for all hours. New Bern (Figure 28) has the best identification overall, with all month mornings having identification rates greater than 60%, and all month nights greater than 40%. Day and evening sample sizes (Figure 29) had less than 10 cases except for December evenings, but all hours other than morning and night had identification rates greater than 40% except for August evenings, which failed to have any observed fog cases with probabilities greater than the 75th percentile of the false alarm probabilities.

Day and evening cases at all sites are difficult to assess because of their lower sample size when compared with morning and night cases. This limits an assessment of

the utility of this method without using a larger historical timespan or coupling a nearby site with better data integrity.

     If a probability threshold using the 75th percentile of false alarms was used in practice, it would present a significant challenge for forecasters as a stand-alone tool. Because there is still a 25% chance of a false alarm, this would indicate that 91.25 days of the year would be incorrectly identified as having fog. However, a 25% failure rate when combined with traditional meteorological analyses could yield accurate results for sites exhibiting a larger sample size than those depicted here. The method could be used in an automated system if a companion fog discriminator were included to rule out obvious false alarms, like in cases where humidity is below 90%.

Chapter 4: Conclusions

The results do not solve the challenges of fog forecasting, but they have shed light on (1) regional conditions favorable for fog formation and (2) challenges in creating a probability of fog formation through an event-based climatology. The results offer a diagnostic tool for assessing fog formation when few resources are available. In that respect, it has accomplished the goals of offering a low-cost method using only readily available observation data. Despite outliers and small sample sizes, there is a separation of probability values between fog and non-fog occurrences when using the 75th percentile of false alarms as a threshold. This suggests that in conjunction with other resources, combined climatology probabilities could serve as a diagnostic tool for fog detection.

Further research could greatly enhance the accuracy of this technique as a standalone tool. The probability tables could be verified further by testing them on nearby stations. This would establish more integrity in the tables by offering additional test cases. The inclusion of snow cover data and precipitation induced fog types would provide more reliable use cases throughout the year for sites.

One method of improving the overall accuracy could use numerical modeling to find a weight of each variable's contribution to fog formation. The weights could then be used to further separate the difference in probabilities between a fog event and a false alarm. One could also seek to combine regional data to increase the sample size and thus the bin sizes, which could similarly allow for weighting of single variable contributions to the overall probability. The site-based analysis of this project would also be ideal for a neural network if it were extended to statewide monitoring (to increase the number of input nodes). The large available ASOS archive makes this project suitable for many machine-

learning techniques, which could further increase the gap between false alarms and actual fog occurrences. Real-time monitoring with predictive methods, like the autoregressive integrated moving average, could help predict future hourly conditions which could then be cross-referenced with the provided tables to detect fog. Coupled with a machine-learning algorithm, a real-time predictive monitor could continuously improve results over time.

REFERENCES

American Meteorological Society, 2015: Glossary of Meteorology. *American Meteorology Society*,. http://glossary.ametsoc.org/ (Accessed October 12, 2015).

Ellrod, G., 2002: ESTIMATION OF LOW CLOUD BASE HEIGHTS AT NIGHT FROM SATELLITE INFRARED AND SURFACE TEMPERATURE DATA. *National Weather Digest*, **26**, 39–44.

Ellrod, G. P., 1995: Advances in the detection and analysis of fog at night using GOES Multispectral infrared imagery. *Weather and Forecasting*, **10**, 606–619, doi:10.1175/1520-0434(1995)010<0606:aitdaa>2.0.co;2.

Gerber, H. E., 1981: Microstructure of a radiation fog. *Journal of the Atmospheric Sciences*, **38**, 454–458, doi:10.1175/1520-0469(1981)038<0454:moarf>2.0.co;2.

Golding, B. W., 1993: A Study of the Influence of Terrain on Fog Development. *Monthly Weather Review*, **121**, 2529–2541, doi:10.1175/1520-0493(1993)121<2529:asotio>2.0.co;2.

Gultepe, I., M. Pagowski, and J. Reid, 2007: A Satellite-Based Fog Detection Scheme Using Screen Air Temperature. *Weather and Forecasting*, **22**, 444–456, doi:10.1175/waf1011.1.

Meyer, M. B., and G. G. Lala, 1990: Climatological Aspects of Radiation Fog Occurrence at Albany, New York. *Journal of Climate*, **3**, 577–586, doi:10.1175/1520-0442(1990)003<0577:caorfo>2.0.co;2.

Oliver, C., 2013: Fog Related Crashes - Statewide Study of Fog Related Crashes in North Carolina. *Traffic Safety Unit, North Carolina Department of Transportation*.

Tardif, R., and R. M. Rasmussen, 2007: Event-Based Climatology and Typology of Fog in the New York City Region. *Journal of Applied Meteorology and Climatology*, **46**(8), 1141–1168. doi:10.1175/jam2516.1

van der Velde, I. R., G. J. Steeneveld, B. G. J. Wichers Schreur, and A. A. M. Holtslag, 2010: Modeling and Forecasting the Onset and Duration of Severe Radiation Fog under Frost Conditions. *Monthly Weather Review*, **138**, 4237–4253, doi:10.1175/2010mwr3427.1.

Westcott, N. E., 2007: Some Aspects of Dense Fog in the Midwestern United States. *Weather and Forecasting*, **22**, 457–465, doi:10.1175/waf990.1.

B. Zhou, and J. Du, 2010: Fog Prediction from a Multimodel Mesoscale Ensemble Prediction System. *Weather and Forecasting*, **25**, 303–322, doi:10.1175/2009waf2222289.1.

1998: *Automated Surface Observing System Users Guide*. National Oceanic and Atmospheric Administration.

2012: Fog. *American Meteorological Society Glossary of Meteorology*. http://glossary.ametsoc.org/wiki/Fog (Accessed December 15, 2015).

Appendix: Figures
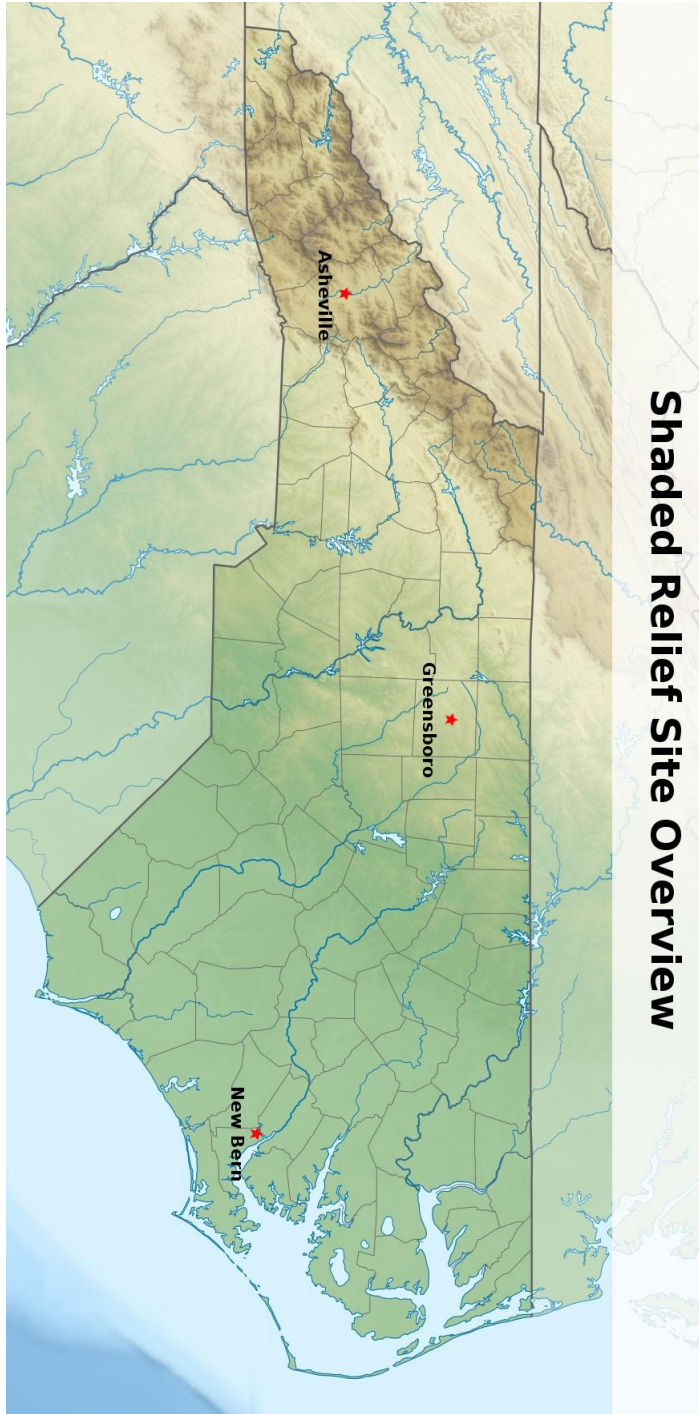
Figure 1: Site Locations and Geography
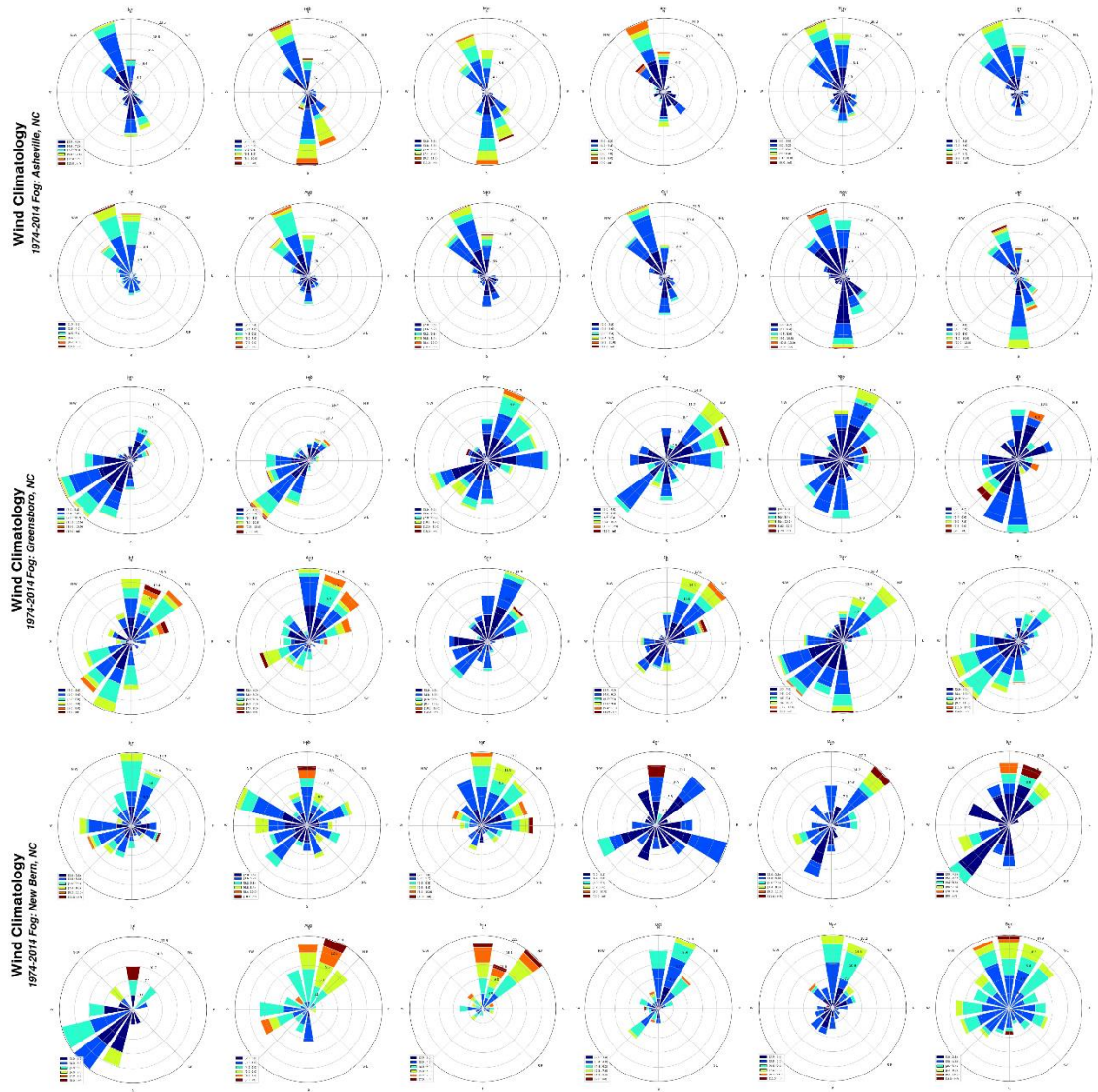
Figure 2: All Sites – Annual Wind Climatology at Fog Onset

Wind Climatology
1974-2014 Greensboro, NC
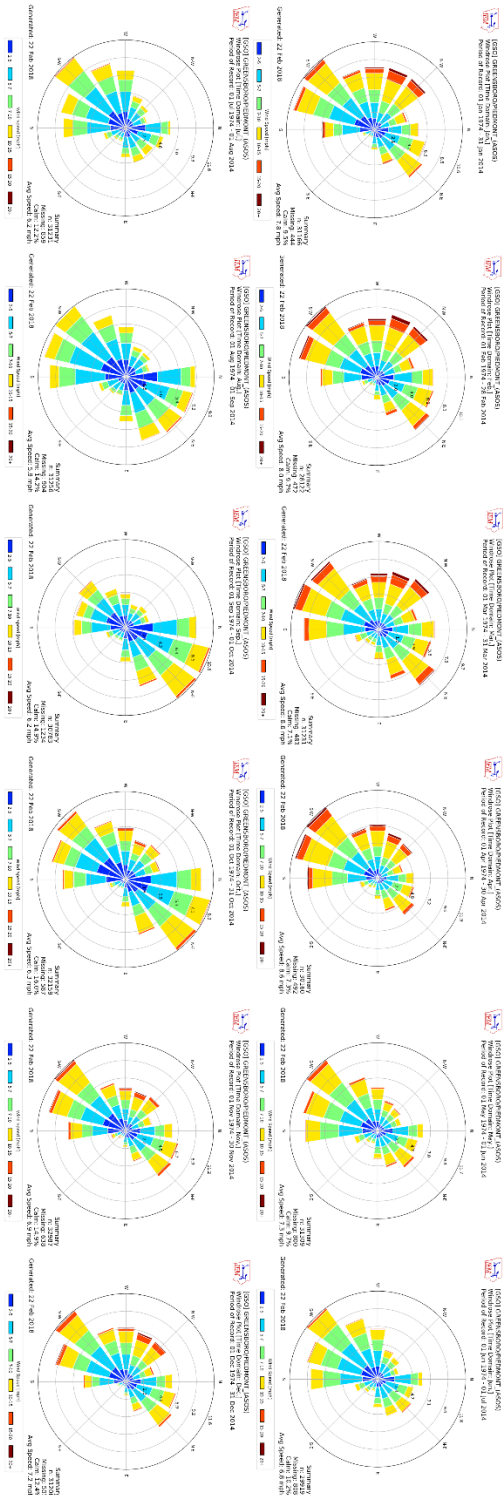
Figure 3: Greensboro, NC – Annual Wind

Wind Climatology
1974-2014 New Bern, NC

Figure 4: New Bern, NC – Annual Wind Climatology (Wind roses courtesy of Iowa Environmental Mesonet)
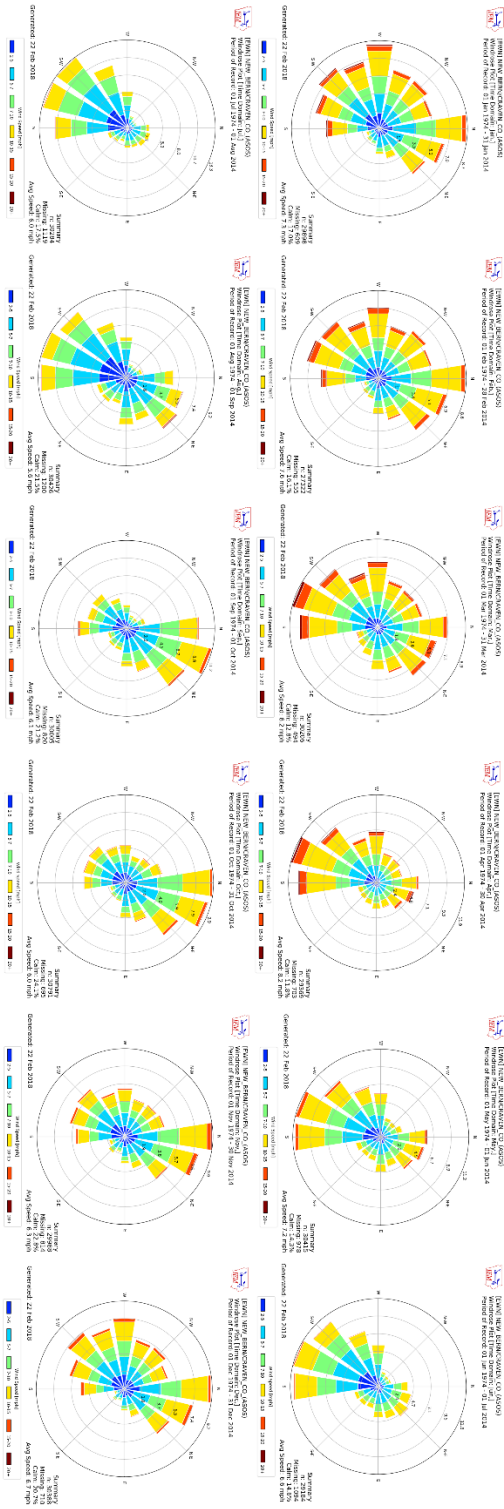
Wind Climatology
1974-2014 Asheville, NC
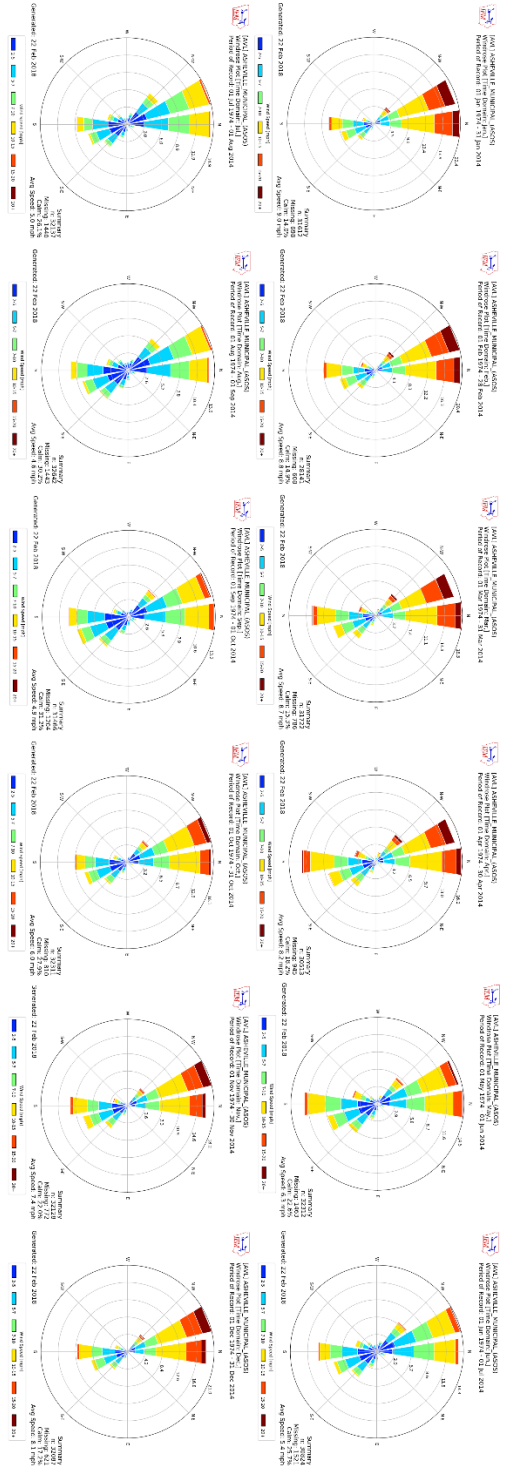
Figure 5: Asheville, NC – Annual Wind Climatology (Wind roses courtesy of Iowa Environmental Mesonet)
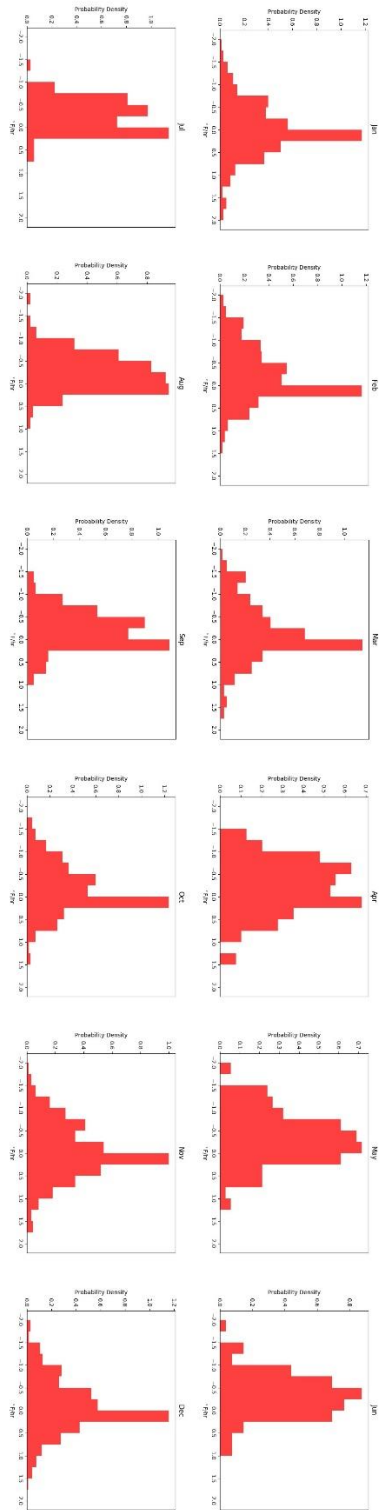
Figure 6: Greensboro, NC – Annual dT Preceding Fog Onset

6hr ΔT Climatology
1974-2014 Fog: New Bern,NC
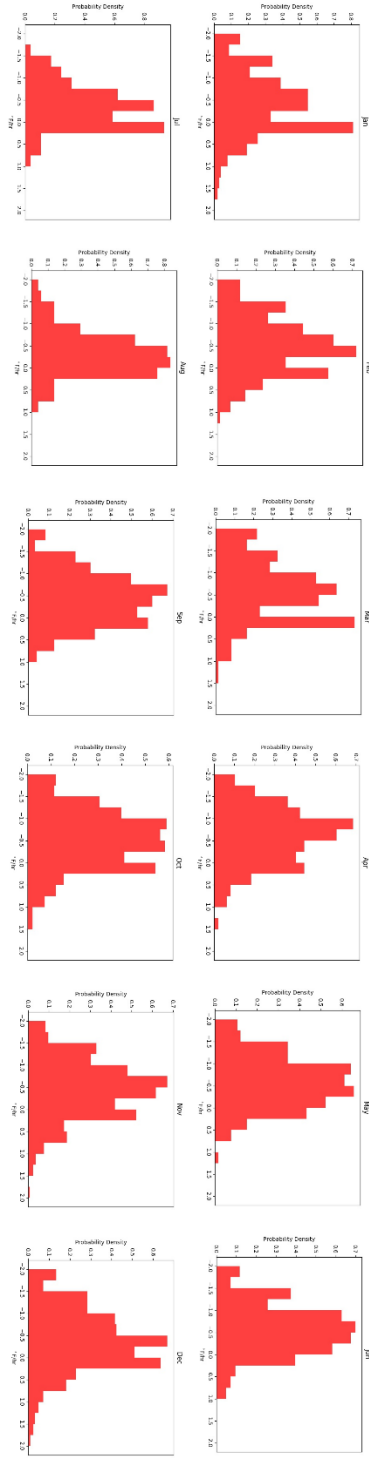
Figure 7: New Bern, NC – Annual dT Preceding Fog Onset

6hr ΔT Climatology
1974-2014 Fog: Asheville,NC
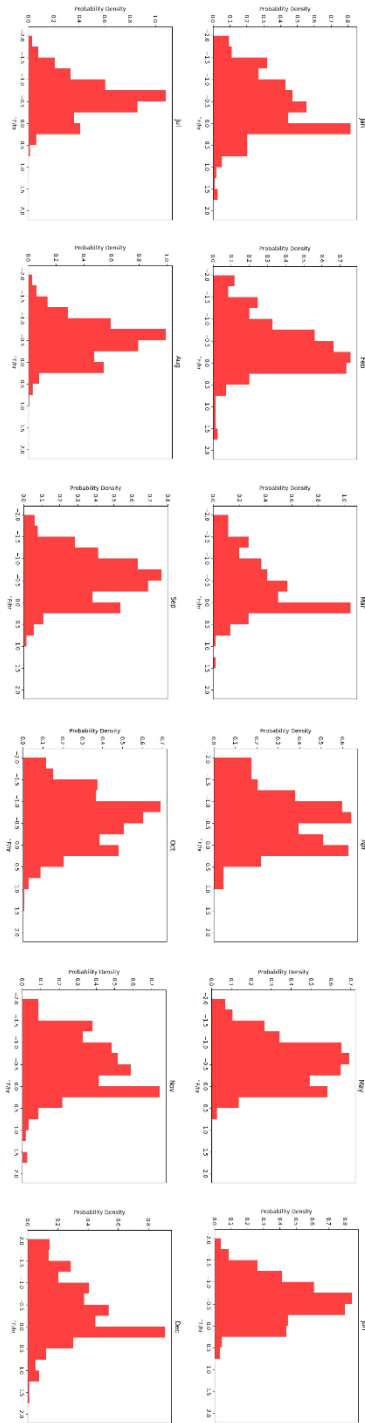
Figure 8: Asheville, NC – Annual dT Preceding Fog Onset

6hr ΔTdd Climatology
1974-2014 Fog: Asheville,NC
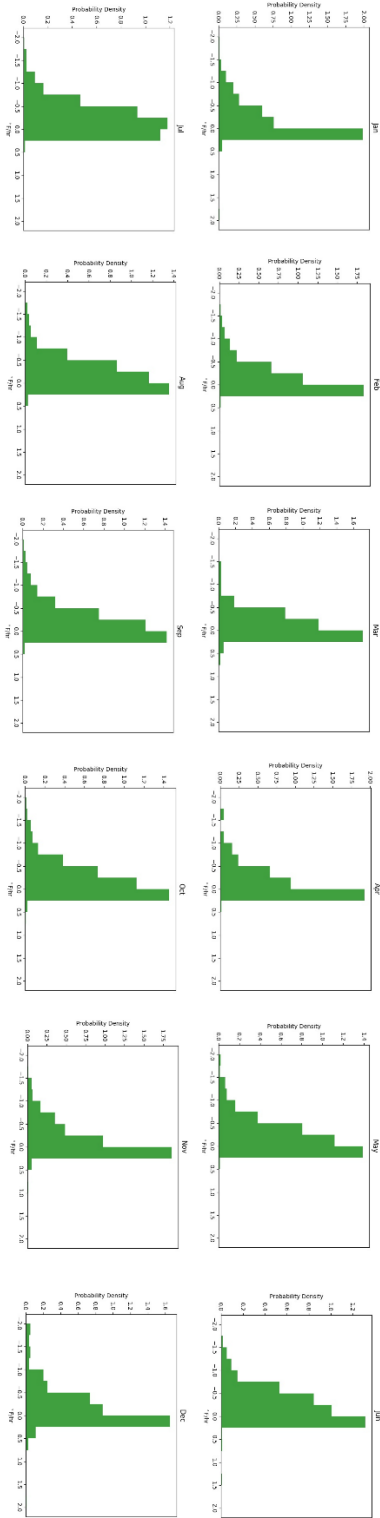
Figure 9: Asheville, NC – Annual 6hr dTdd Preceding Fog Onset
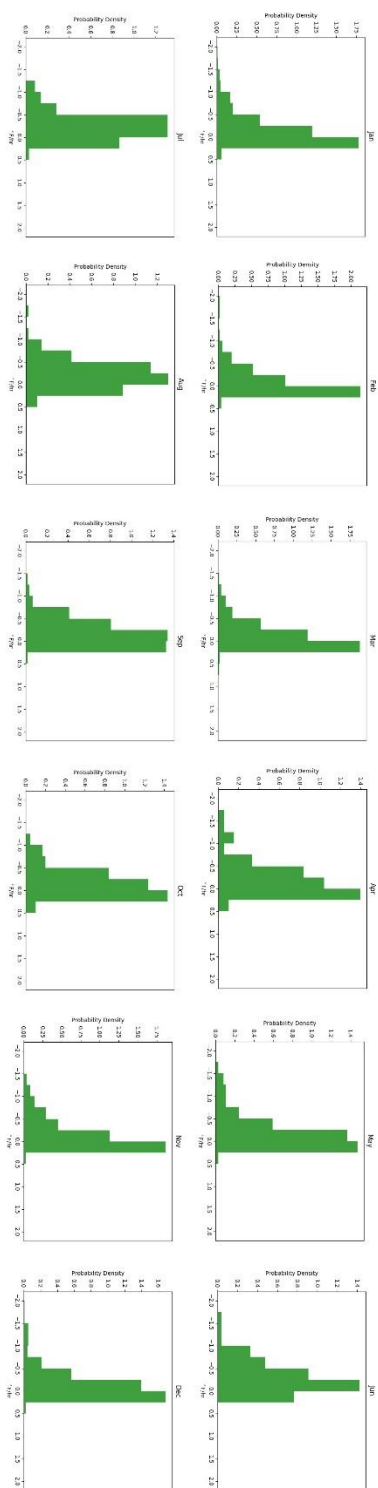
Figure 10: Greensboro, NC – Annual 6hr dTdd Preceding Fog Onset

6hr ΔTdd Climatology
1974-2014 Fog: New Bern,NC
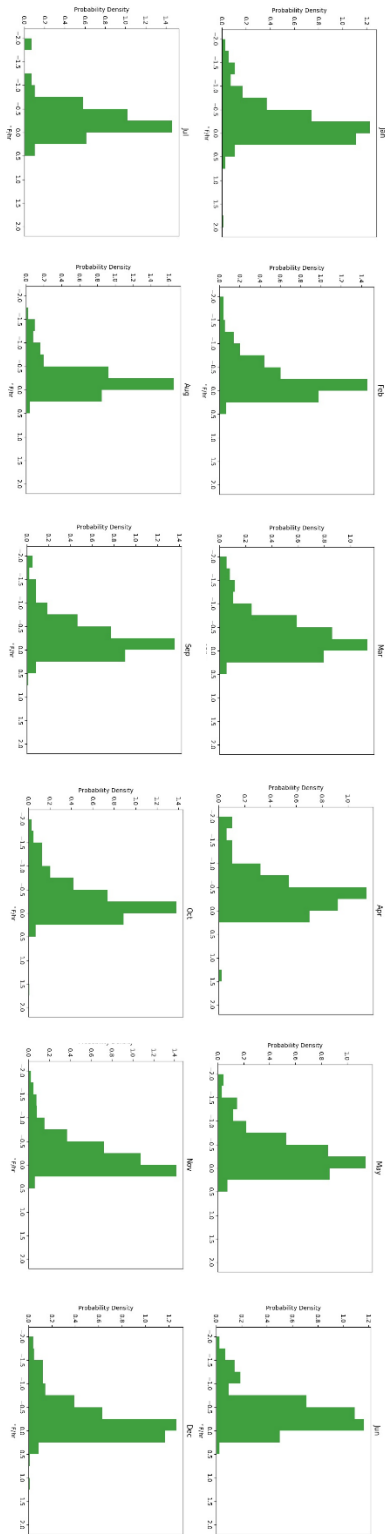
Figure 11: New Bern, NC – Annual 6hr dTdd Preceding Fog Onset

Asheville, 6 Hour Precip (in) Preceding Fog Onset (EST)
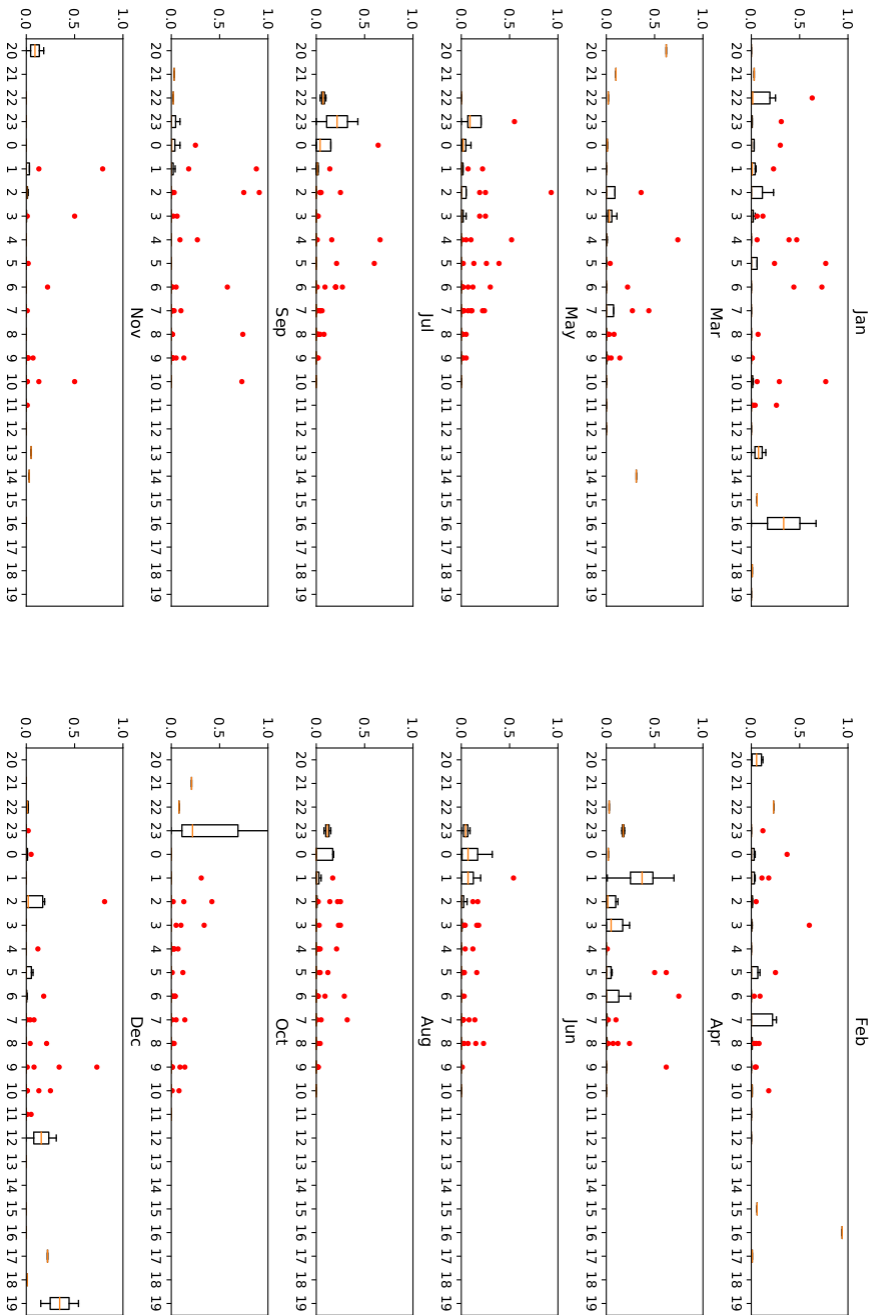
Figure 12: Asheville, NC – Annual 6hr Precipitation Preceding Fog Onset

Asheville, 12 Hour Precip (in) Preceding Fog Onset (EST)
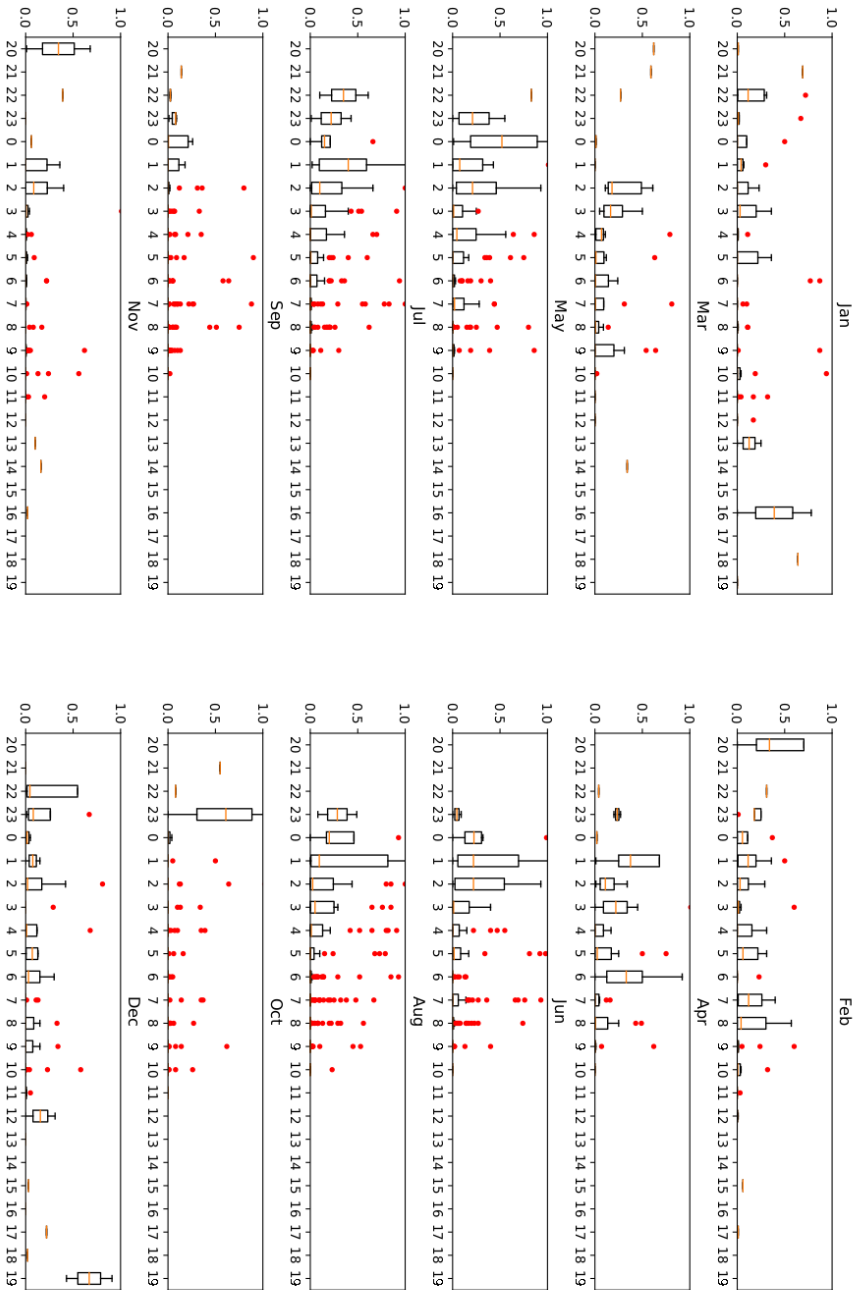
Figure 13: Asheville, NC – Annual 12hr Precipitation Preceding Fog Onset

34

Asheville, 24 Hour Precip (in) Preceding Fog Onset (EST)
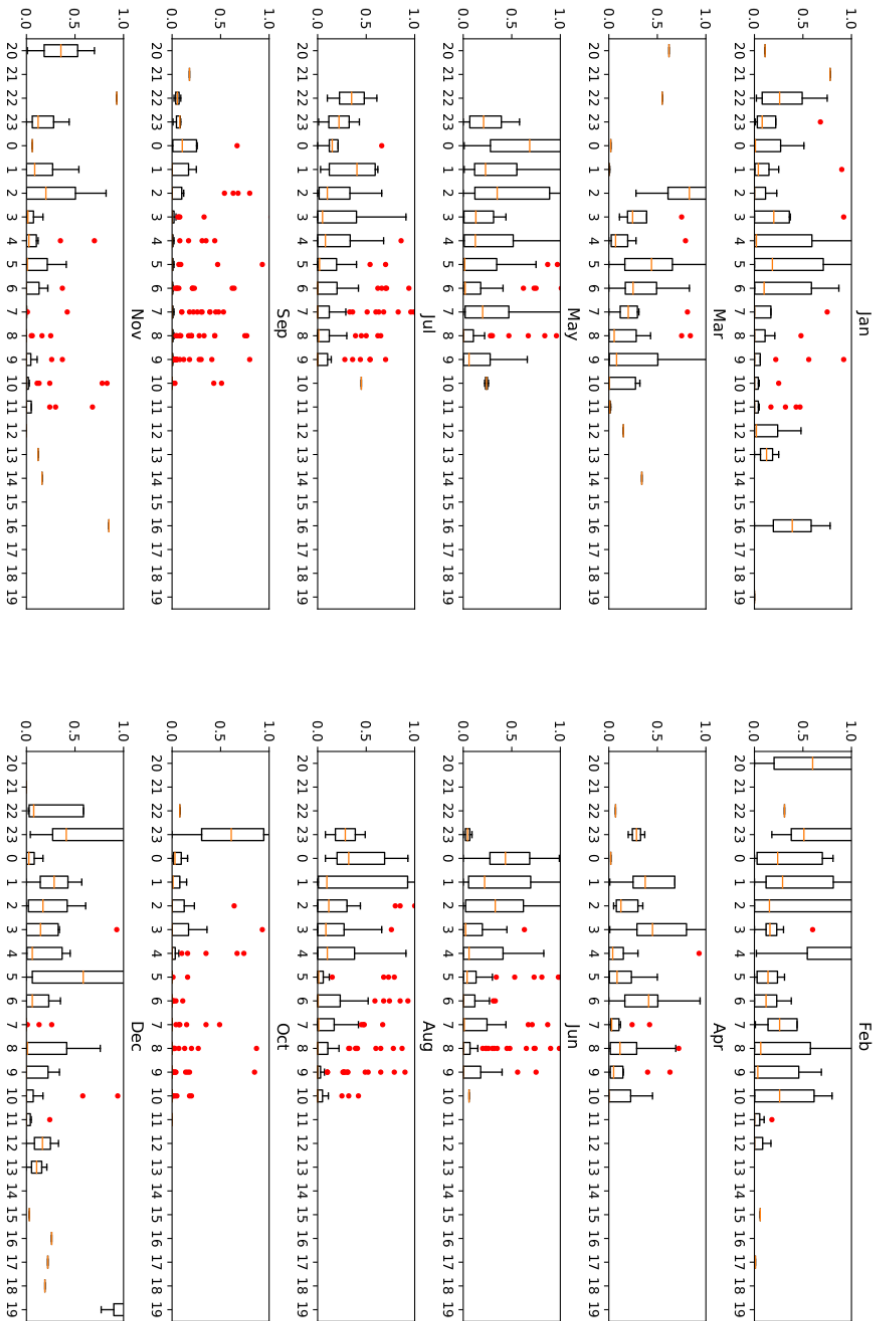
Figure 14: Asheville, NC – Annual 24hr Precipitation Preceding Fog Onset

Greensboro, 6 Hour Precip (in) Preceding Fog Onset (EST)
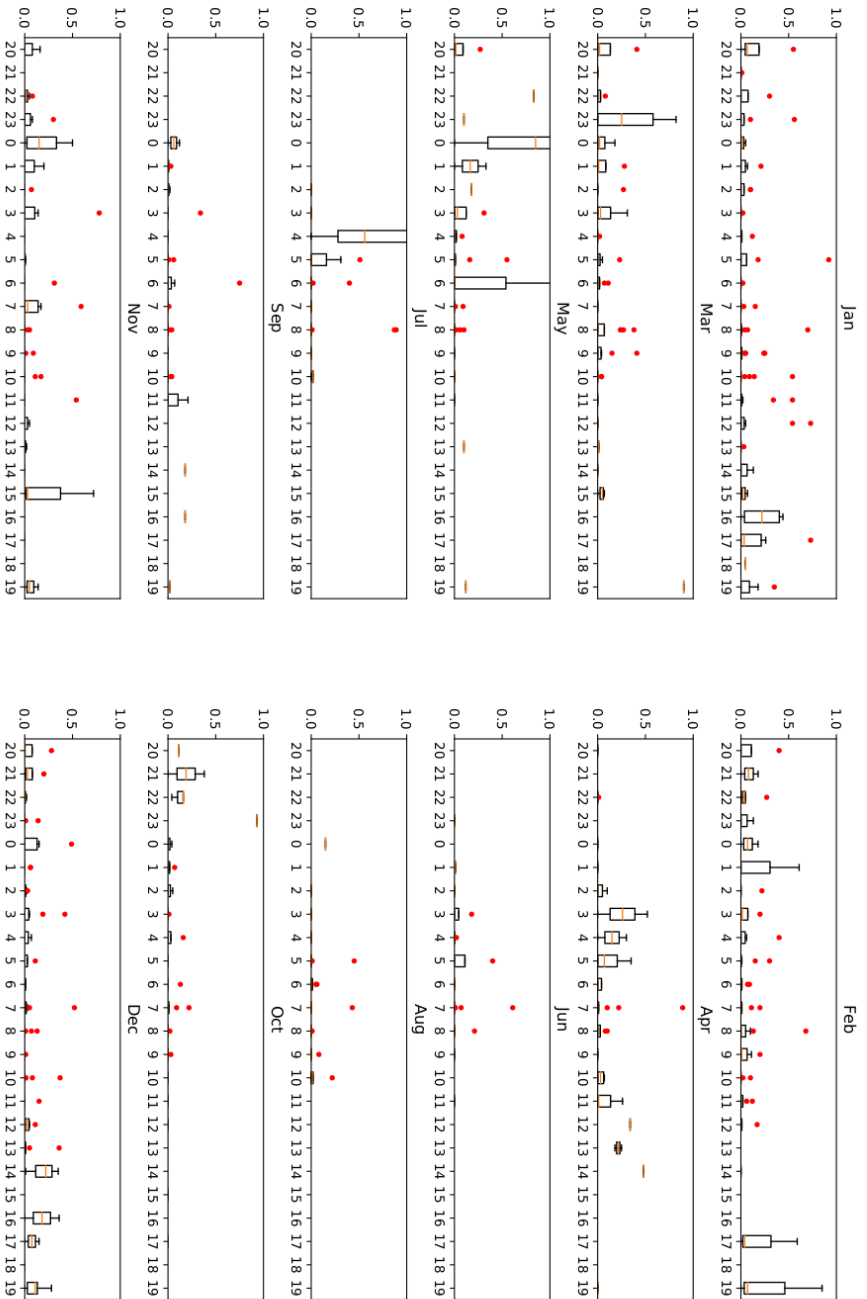
Figure 15: Greensboro, NC – Annual 6hr Precipitation Preceding Fog Onset
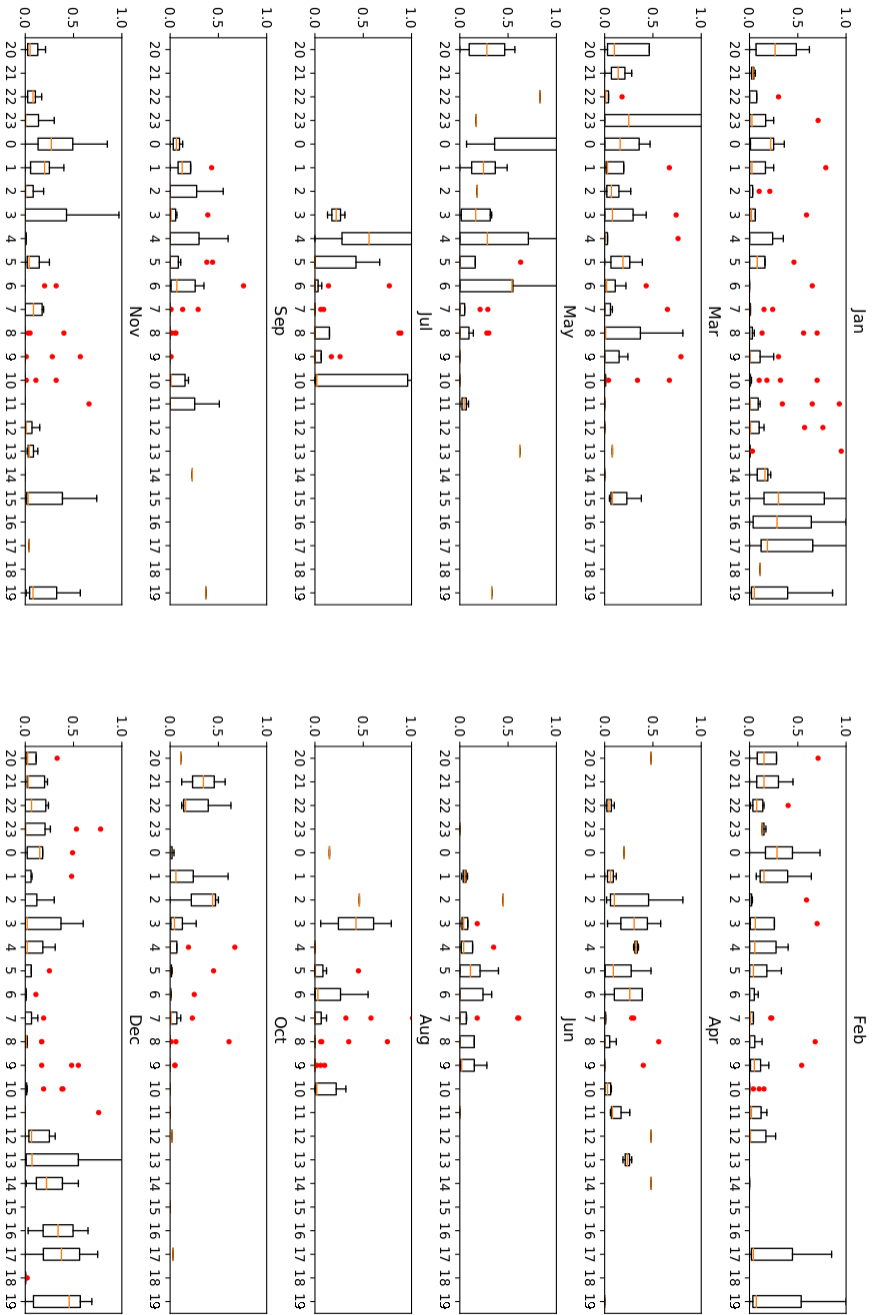
Figure 16: Greensboro, NC – Annual 12hr Precipitation Preceding Fog Onset

Greensboro, 24 Hour Precip (in) Preceding Fog Onset (EST)
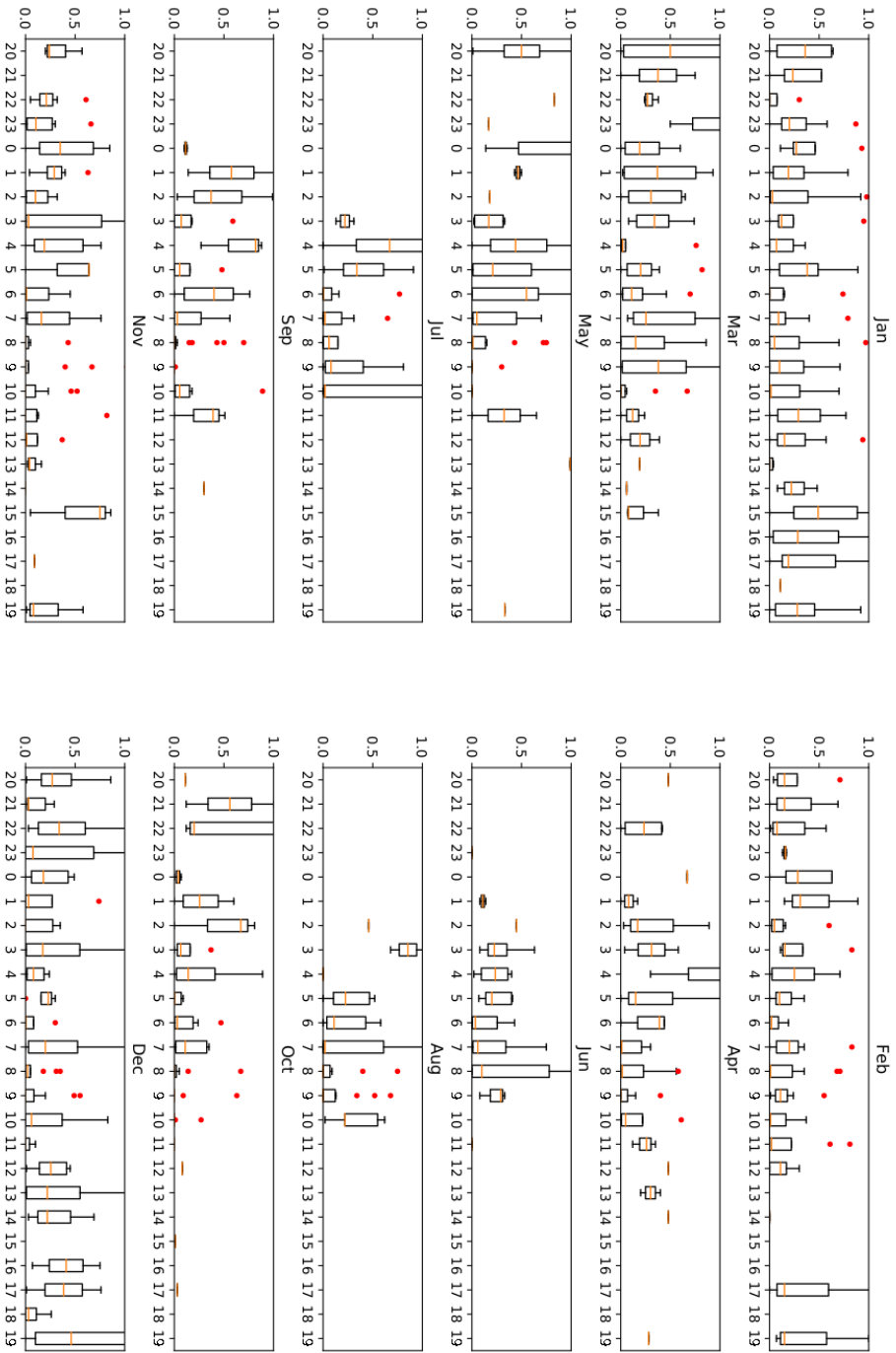
Figure 17: Greensboro, NC – Annual 24hr Precipitation Preceding Fog Onset

New_Bern, 6 Hour Precip (in) Preceding Fog Onset (EST)
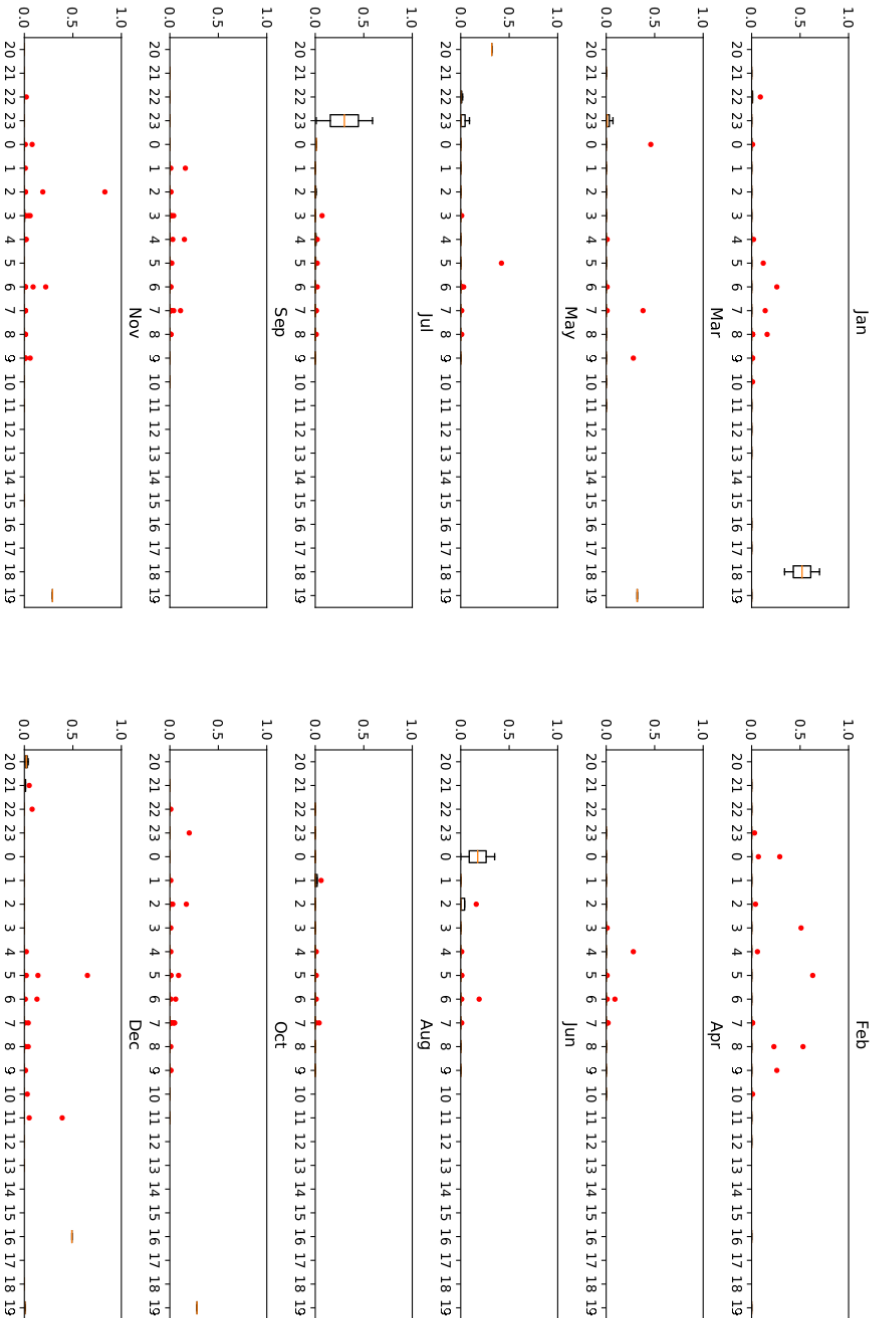
Figure 18: New Bern, NC – Annual 6hr Precipitation Preceding Fog Onset

New_Bern, 12 Hour Precip (in) Preceding Fog Onset (EST)
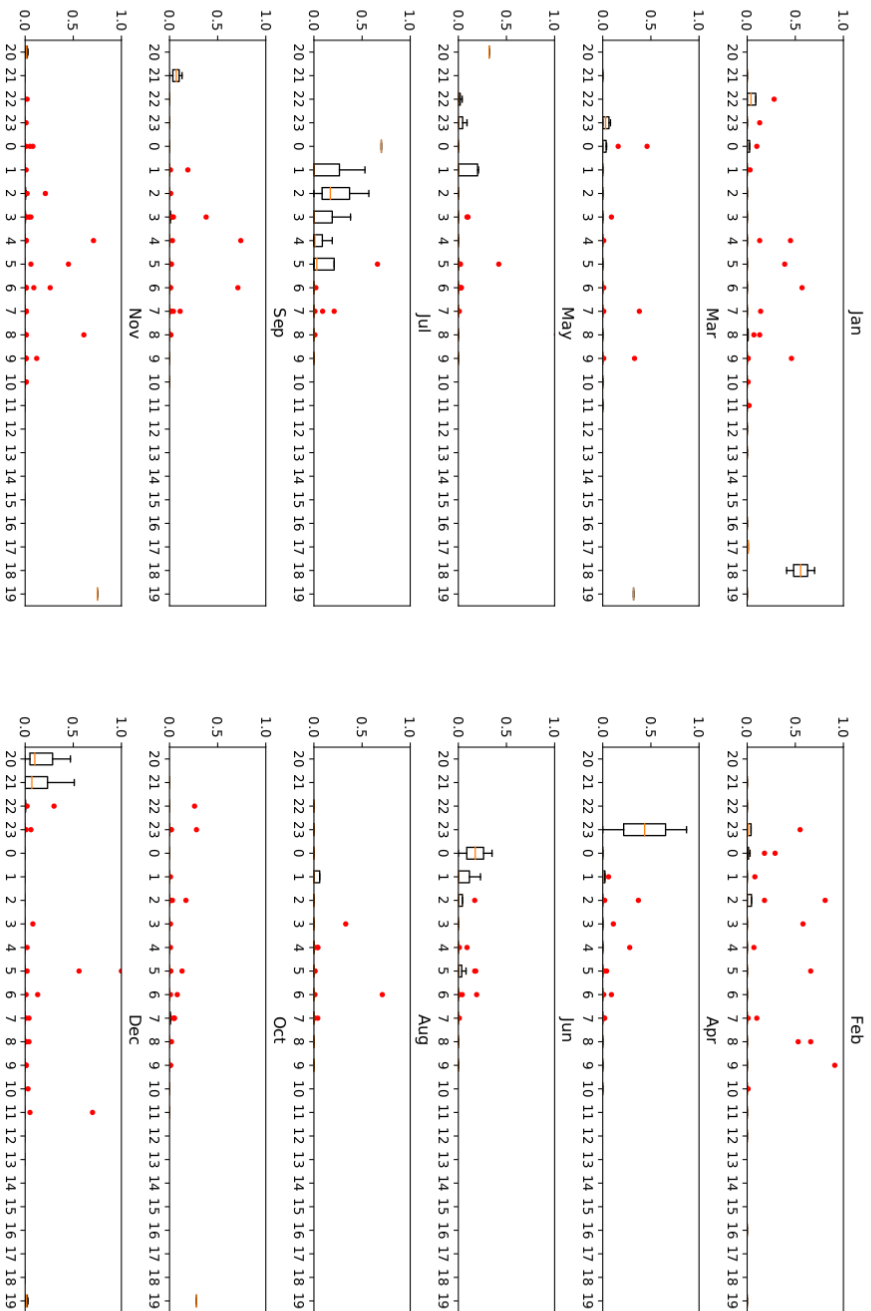
Figure 19: New Bern, NC – Annual 12hr Precipitation Preceding Fog Onset

New_Bern, 24 Hour Precip (in) Preceding Fog Onset (EST)
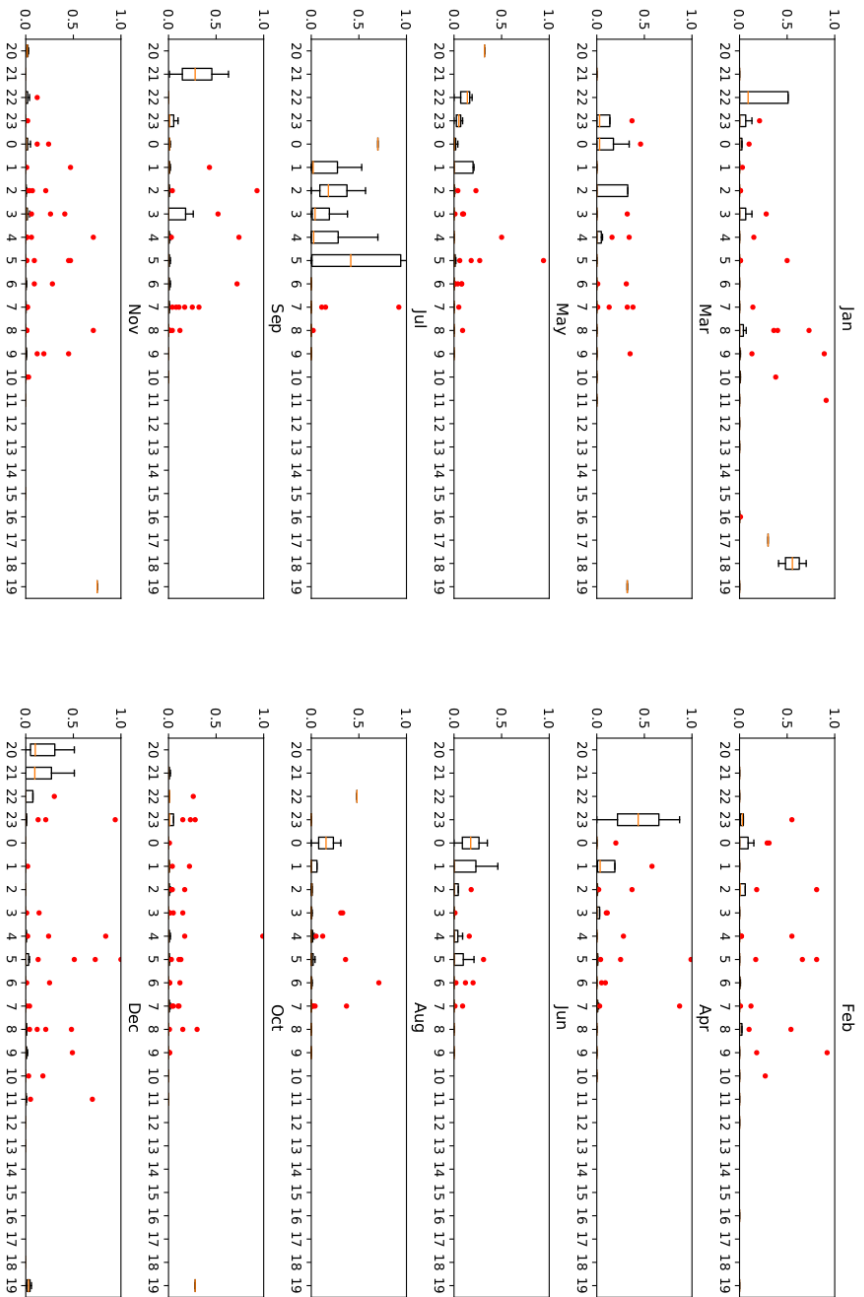
Figure 20: New Bern, NC – Annual 24hr Precipitation Preceding Fog Onset

Asheville Fog Probabilities
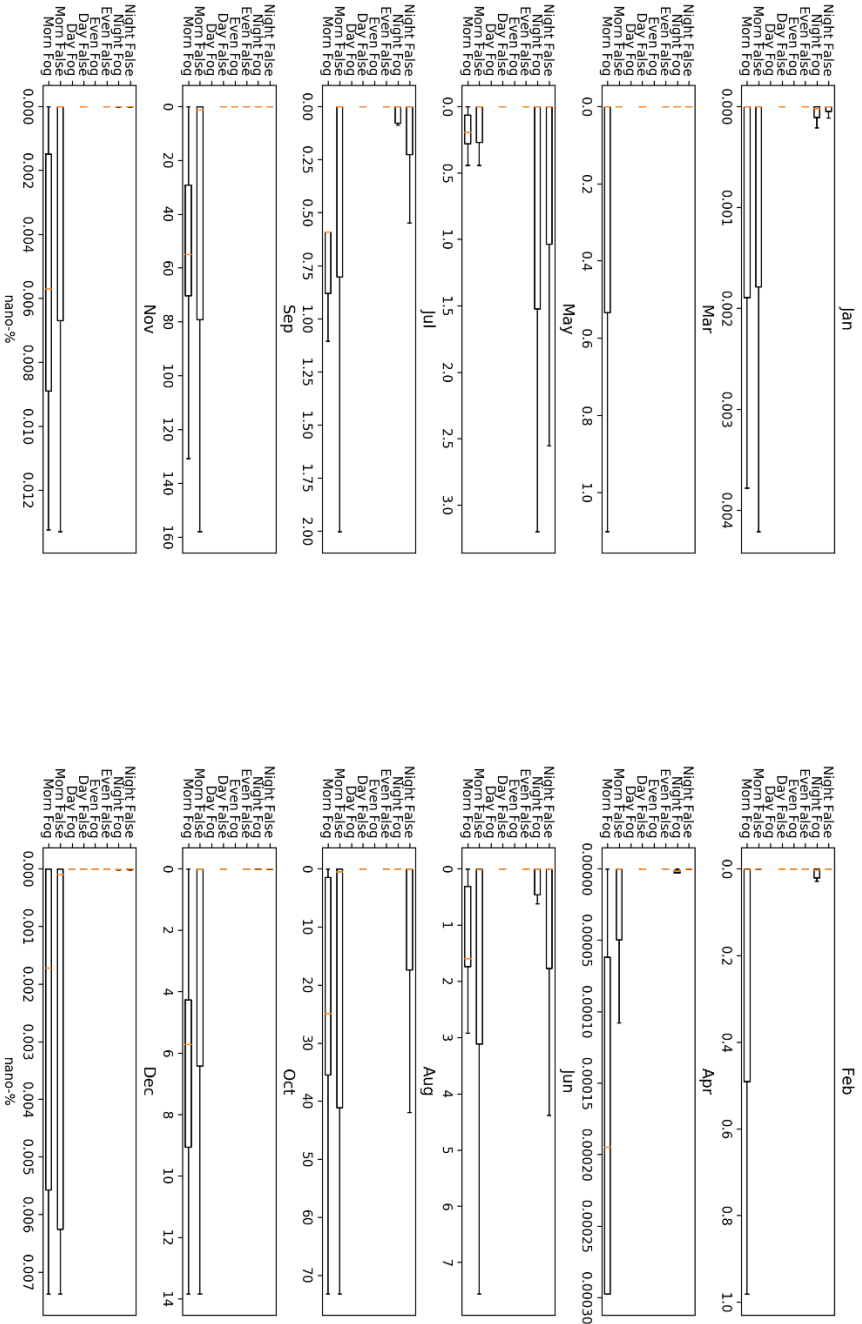
Figure 21: Asheville, NC – 40yr Combined Fog Probabilities
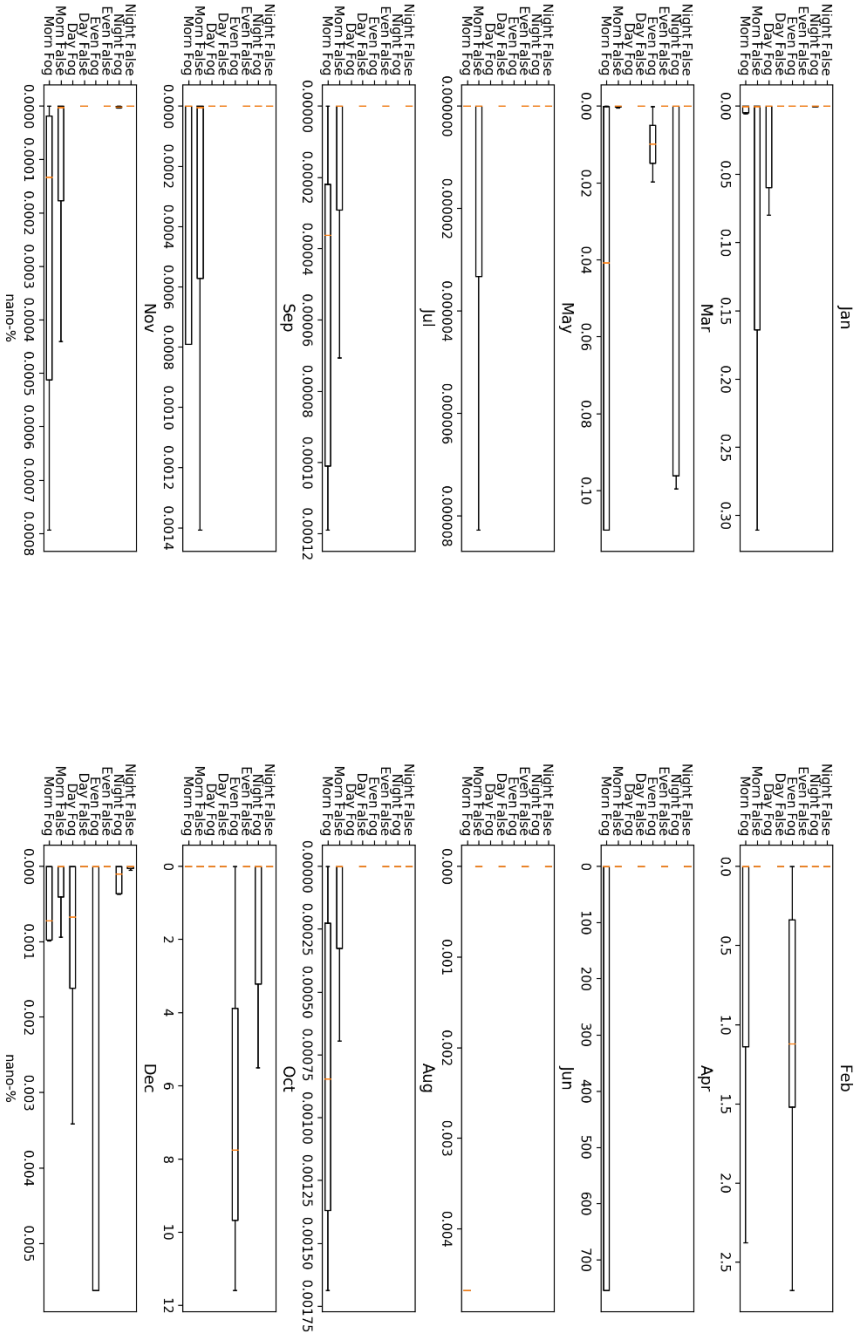
Figure 22: Greensboro, NC – 40yr Combined Fog Probabilities
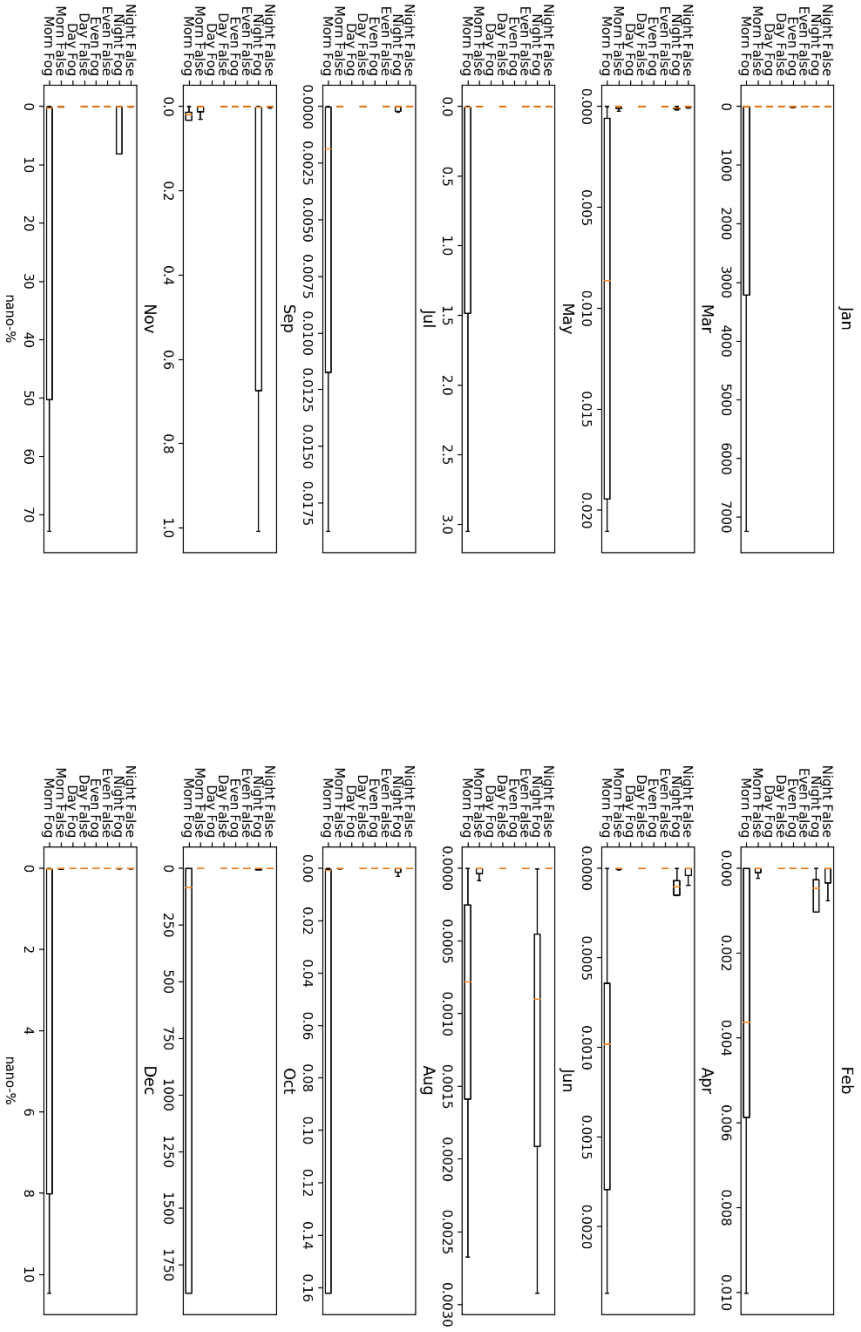
Figure 23: New Bern, NC – 40yr Combined Fog Probabilities
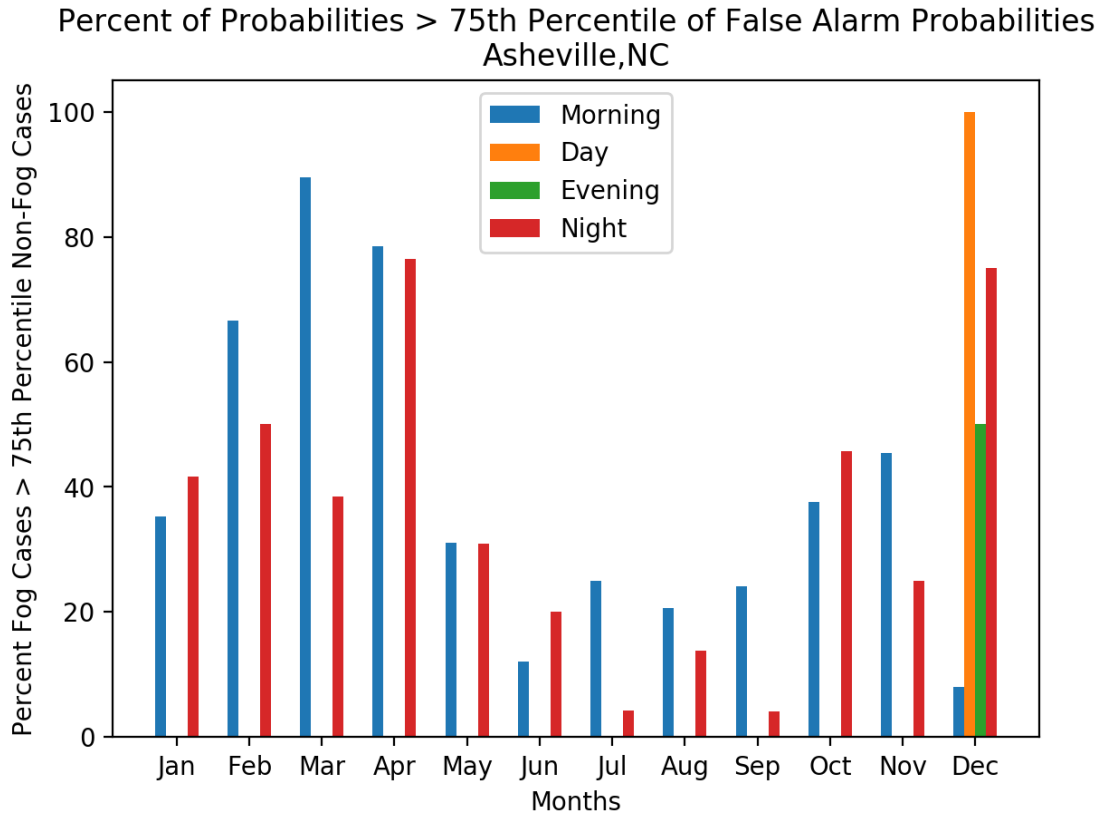
Figure 24: Asheville, NC – Percent of Probabilities Greater than the 75th Percentile of False Alarm Probabilities
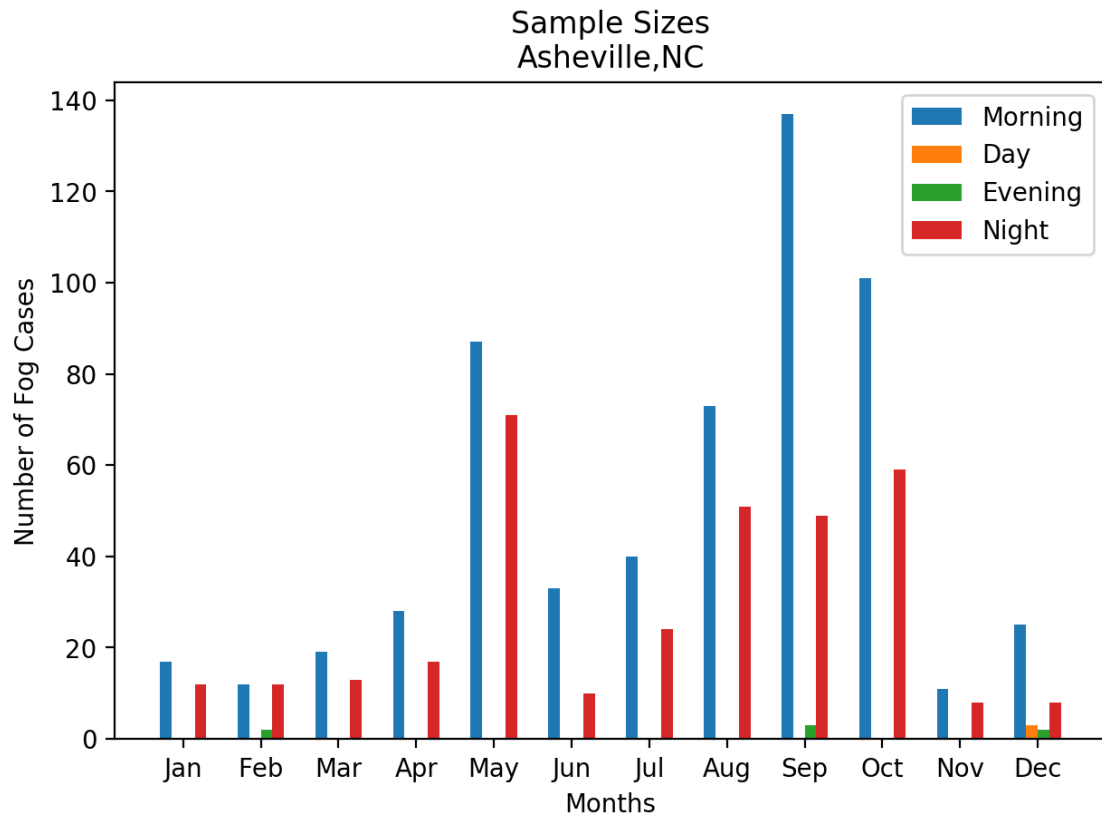
Figure 25: Asheville, NC – 40yr Combined Probability Sample Sizes
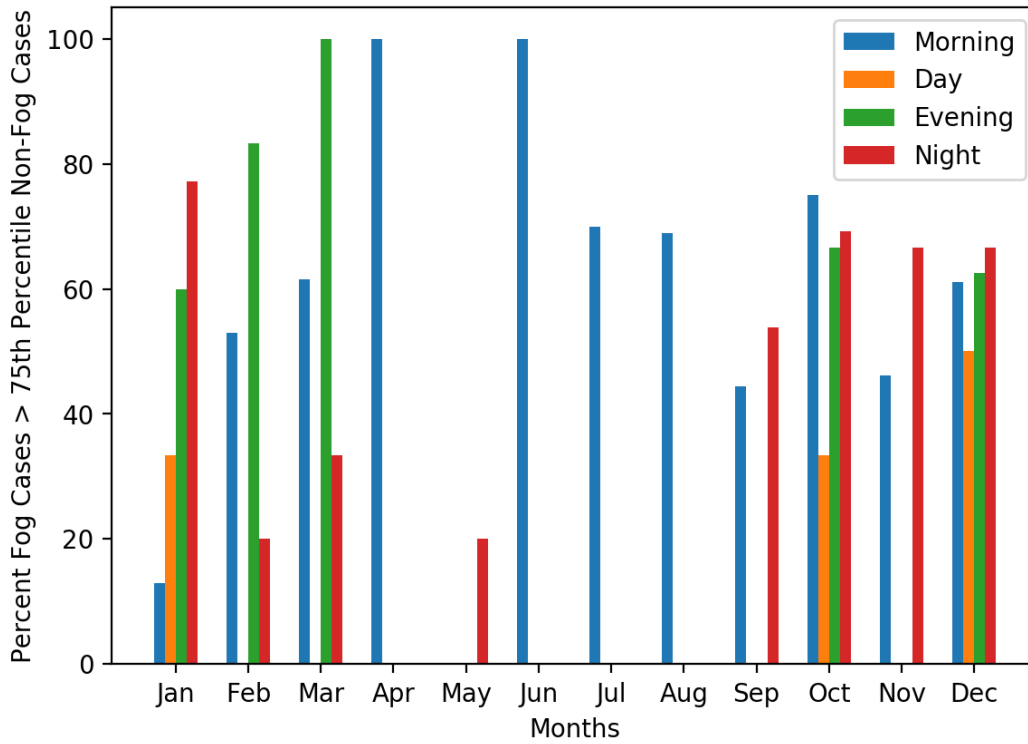
Figure 26: Greensboro, NC – Percent of Probabilities Greater than the 75th Percentile of False Alarm Probabilities
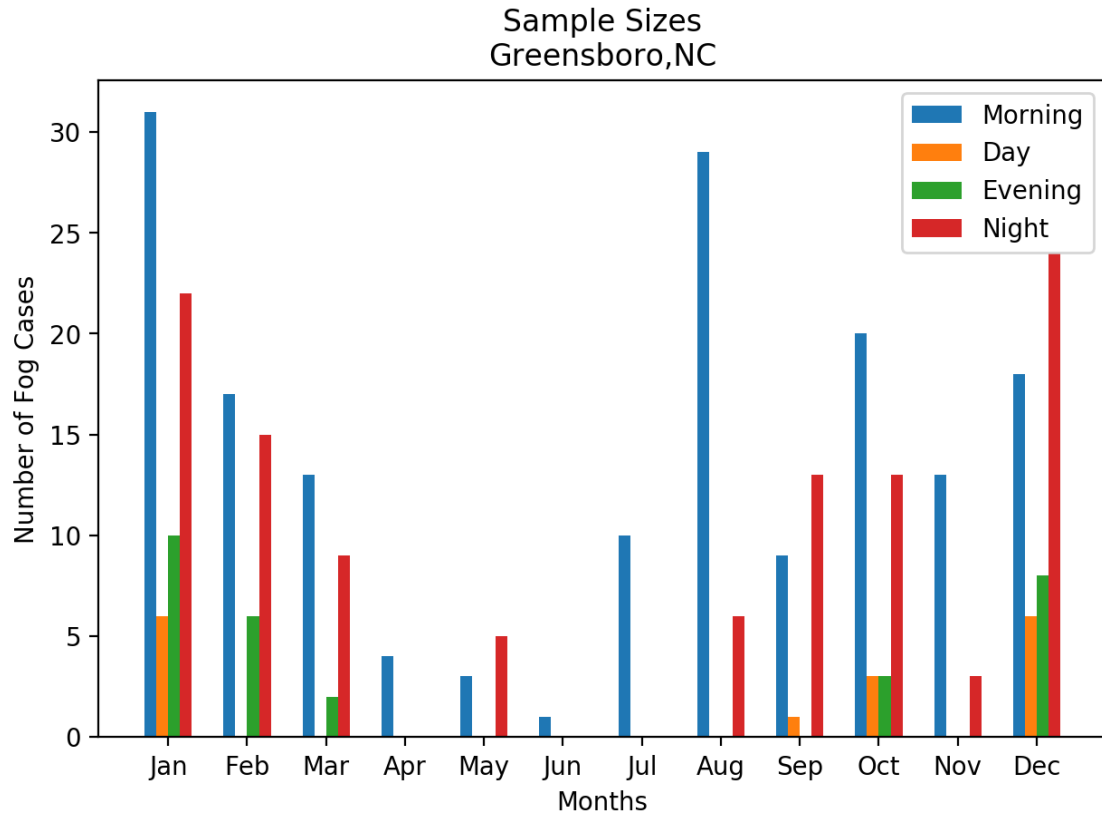
Figure 27: Greensboro, NC – 40yr Combined Climatology Sample Sizes
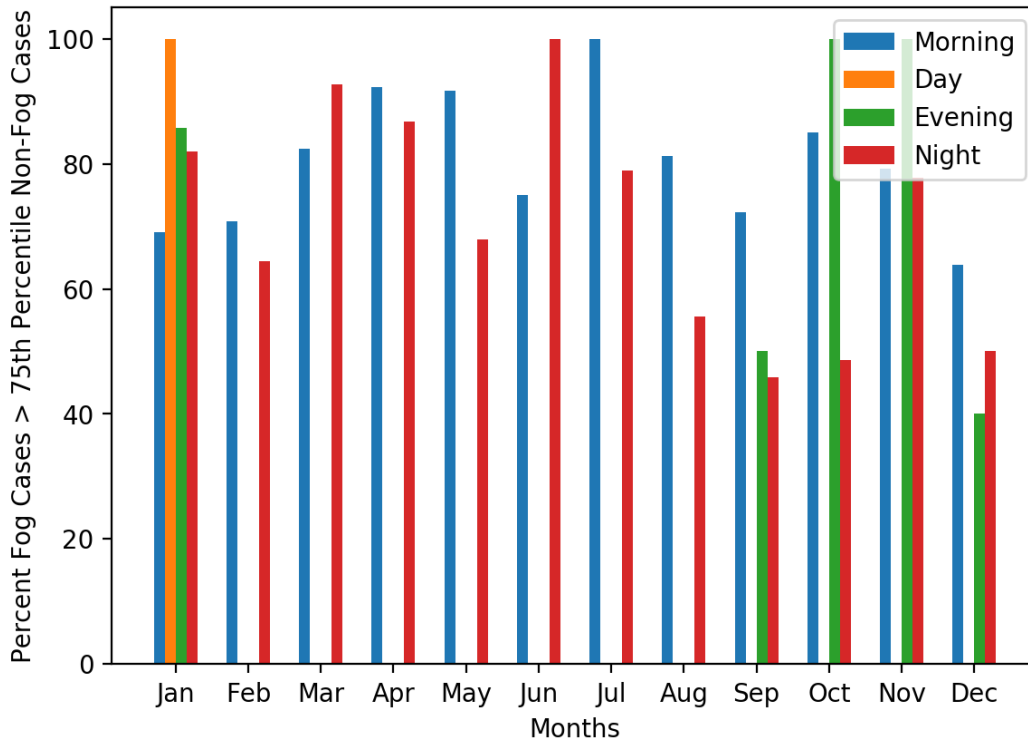
Figure 28: New Bern, NC – Percent of Probabilities Greater than the 75th Percentile of False Alarm Probabilities
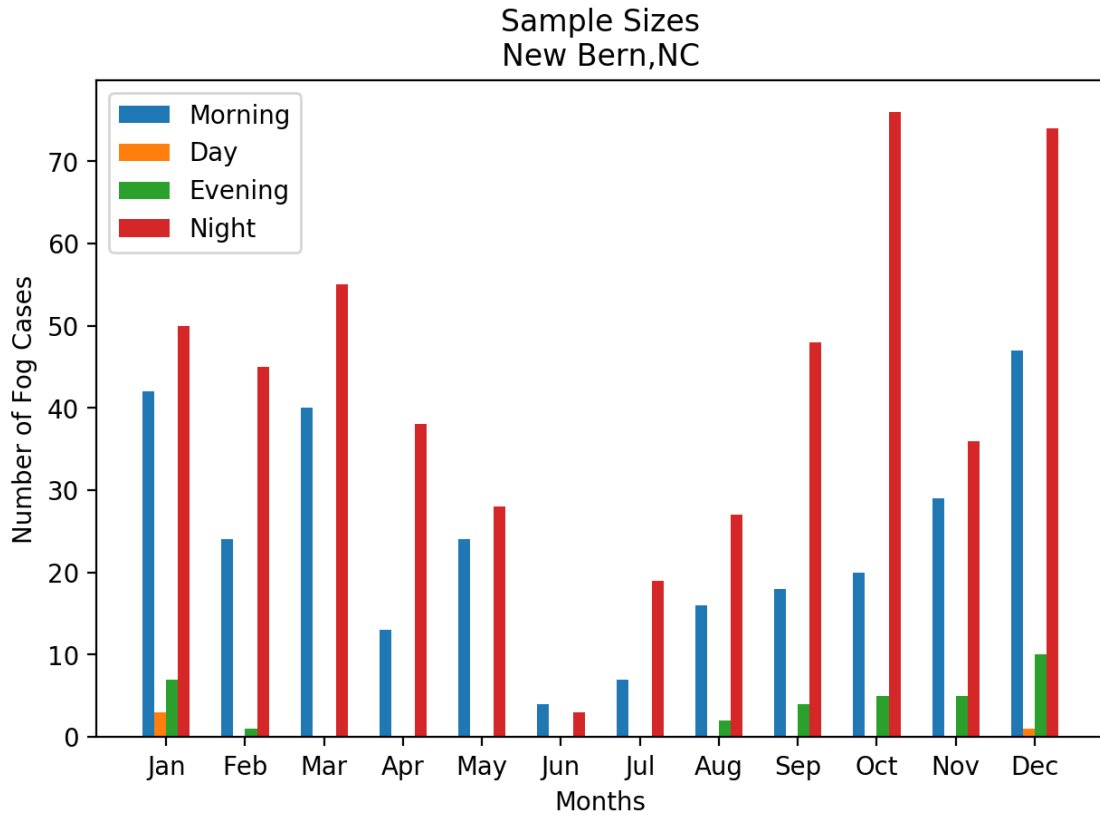
Figure 29: New Bern, NC – 40yr Combined Climatology Probability Sample Sizes